AD-A068 552   NAVAL SURFACE WEAPONS CENTER DAHLGREN LAB VA   F/G 20/3
              ANALYTICAL STUDY ON THE IDEAL RESPONSE OF NORMAL-MODE SHOCK-DEP--ETC(U)
              JUL 78   W MOCK, W H HOLT

UNCLASSIFIED   NSWC/DL/TR-3822   NL

| OF |
AD
A068552

END
DATE
FILMED
6-79
DDC

REPORT DOCUMENTATION PAGE		READ INSTRUCTIONS BEFORE COMPLETING FORM
1. REPORT NUMBER NSWC/DL TR-3822	2. GOVT ACCESSION NO.	3. RECIPIENT'S CATALOG NUMBER
4. TITLE (and Subtitle) ANALYTICAL STUDY ON THE IDEAL RESPONSE OF NORMAL-MODE SHOCK-DEPOLED PZT FERROELECTRIC CERAMICS WITH RESISTIVE, CAPACITIVE, AND INDUCTIVE LOADS		5. TYPE OF REPORT & PERIOD COVERED Final
		6. PERFORMING ORG. REPORT NUMBER
7. AUTHOR(s) W. Mock, Jr. W. H. Holt		8. CONTRACT OR GRANT NUMBER(s)
9. PERFORMING ORGANIZATION NAME AND ADDRESS Naval Surface Weapons Center (G30) Dahlgren, VA 22448		10. PROGRAM ELEMENT, PROJECT, TASK AREA & WORK UNIT NUMBERS 6233N/S32382/ WF32382501/DF29
11. CONTROLLING OFFICE NAME AND ADDRESS Naval Air Systems Command Washington, DC 20360		12. REPORT DATE July 1978
		13. NUMBER OF PAGES 64
14. MONITORING AGENCY NAME & ADDRESS(if different from Controlling Office)		15. SECURITY CLASS. (of this report) UNCLASSIFIED
		15a. DECLASSIFICATION/DOWNGRADING SCHEDULE

16. DISTRIBUTION STATEMENT (of this Report)

Approved for public release; distribution unlimited.

17. DISTRIBUTION STATEMENT (of the abstract entered in Block 20, if different from Report)

18. SUPPLEMENTARY NOTES

19. KEY WORDS (Continue on reverse side if necessary and identify by block number)

Ferroelectric ceramics   Ferroelectric power supply
Shock waves   Pulse power
Shock-depoled ferroelectrics

20. ABSTRACT (Continue on reverse side if necessary and identify by block number)

Electrical equations have been derived for the ideal response of normal-mode shock-depoled PZT ferroelectric ceramics with resistive, capacitive, and inductive loads. It was assumed in the analysis that charge was released from the PZT material completely and instantaneously at the shock front. Both rectangular and hollow-cylinder shapes were considered for the PZT unit. Expressions for the charge, voltage, current, and energy in the circuit were obtained for times during and after the traversal of the unit by the shock front. These results and the electrical properties of shock-depoled

(see back)

DD FORM 1473 EDITION OF 1 NOV 65 IS OBSOLETE
1 JAN 73
S/N 0102-LF-014-6601

79 05 11 027

(20)

PZT 56/44 ceramics were used to estimate the geometrical size of PZT units in single-shot pulsed power supplies for energy converters with resistive and capacitive input characteristics.
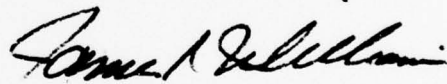
FOREWORD

In this report, electrical expressions have been obtained for the ideal response of normal-mode shock-depoled PZT ferroelectric ceramics with resistive, capacitive, and inductive loads. These results have application in the design of single-shot ferroelectric pulse power supplies. Funding for this work was provided by NAVAIR Task No. A350-3500/004C/6WTW27-001.

This report has been reviewed and approved by C. A. Cooper, Head, Gun Systems and Munitions Division.

Released by:

CDR JAMES R. WILLIAMS
Assistant Head for Weapons Systems
Weapons Systems Department

iii

ACKNOWLEDGMENT

CONTENTS

ILLUSTRATIONS

LIST OF TABLES

I. INTRODUCTION

Shock-excited lead zirconate titanate (PZT) ferroelectric ceramic materials have been used in single-shot pulse power supplies to deliver average powers that range from a few hundred kilowatts to a megawatt in a few microseconds.[1-3] The bound surface charge is released from the poled PZT ceramic as a shock wave passes through it. Previous experimental investigations of charge release phenomena under shock wave compression have been concerned primarily with short-circuit conditions and large resistive loads.[2-4] A few investigations have been reported for capacitive loads[1] and inductive loads.[5] To date a detailed theory has not been developed for the electrical response of a shock-compressed ferroelectric ceramic due to the complicated nature of the depoling process.[2] The purpose of this report is to derive electrical expressions for the response of shock-depoled ferroelectric ceramics with various loads by using simple assumptions for the depoling process. Electrical expressions are obtained for the charge, voltage, current, and energy in the circuit for resistive, capacitive, and inductive loads that range from short-circuit to open-circuit conditions. Plots are presented for these expressions. The results will be useful in estimating the actual response of shock-depoled PZT materials as the magnitude and type of load varies.

PZT ceramic materials are usually depoled in either of two modes: normal mode or axial mode. The shock wave propagates through the PZT material in a direction either perpendicular or parallel to the PZT remanent polarization vector for normal- or axial-mode depoling, respectively. Normal-mode depoling is usually preferred for high-voltage applications since for axial-mode depoling time-dependent electric fields much larger than the dielectric breakdown strength of the PZT material can be generated behind the shock front.[4] In this report, only normal-mode depoling is considered.

The simple assumptions that are made concerning the shock depoling of the PZT material and the two PZT geometries that are considered are given in Section II. Sections III, IV, and V contain the analyses for the resistive, capacitive, and inductive loads, respectively. Geometrical size estimates of PZT units for pulsed power supplies for selected high-voltage energy converters are given in Section VI. Section VII contains the summary.

II. SIMPLIFYING ASSUMPTIONS FOR THE CHARGE RELEASE FROM A SHOCK-DEPOLED PZT UNIT

It is assumed in this analysis that the PZT material responds in what will be called an ideal manner. The assumptions for this type of response are: (1) the shock front is steady and moves with a single shock velocity U, (2) the permittivity of the PZT material is strictly constant (no dielectric relaxation) and equal ahead of and behind the shock front, (3) no electrical breakdown and conduction occur in the PZT material, (4) the PZT material is depoled completely and instantaneously at the shock front with no kinetic effects occurring, (5) the strain behind the shock front is negligible, and (6) once the PZT material comes under shock-wave compression, it remains in that stress state. Although these simplifying assumptions do not hold for all depoling modes, stress values, and electrical load conditions,[4,6,7] experimental results have shown that a stress range exists for some PZT materials in which the simplifying assumptions are approximately valid.[1,8-10]

The two geometrical shapes for the PZT material that are considered in this study are the rectangular PZT unit and the hollow-cylinder PZT unit. A schematic for the normal-mode depoling of a rectangular unit is shown in Figure 1(a). A planar shock wave is produced at one surface of the unit usually by explosive detonation or projectile impact. A schematic for the normal-mode depoling of a hollow-cylinder unit is shown in Figure 1(b). For this unit, a shock wave is produced by axial detonation of a concentric cylinder of explosive located inside the PZT cylinder. The PZT material is usually surrounded with a high-dielectric-strength material (such as alumina-filled epoxy or transformer oil) to reduce the possibility of dielectric breakdown around the edges of the unit under the combined effects of high voltage and stress.[1,3]

For the rectangular PZT unit, the bound surface charge is released in a linear manner by the propagating shock wave. At time t the released charge is

$$q(t) = \begin{cases} P_0 A \dfrac{t}{\tau} \ , & 0 \leqslant t \leqslant \tau \ , \\ \\ P_0 A \ , & t > \tau \ , \end{cases} \qquad (1)$$

where $A = w\ell$ is the electroded area and $\tau = \ell/U$ is the shock transit time. The capacitances behind and ahead of the shock front are given, respectively, by

$$C_1(t) = \frac{A\epsilon}{h} \frac{t}{\tau} \ , \quad 0 \leqslant t \leqslant \tau \ , \qquad (2)$$

2
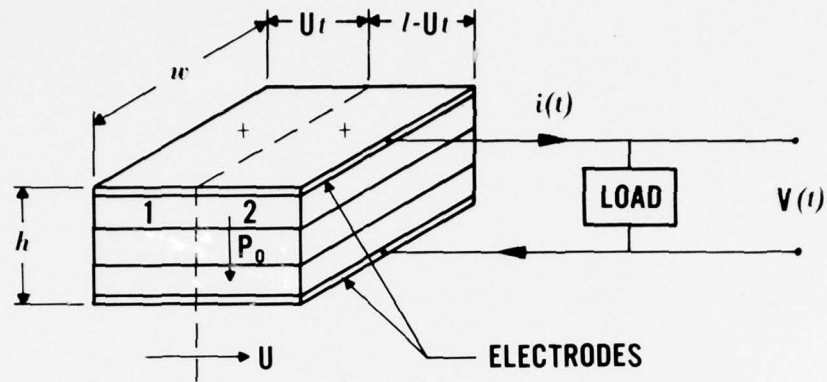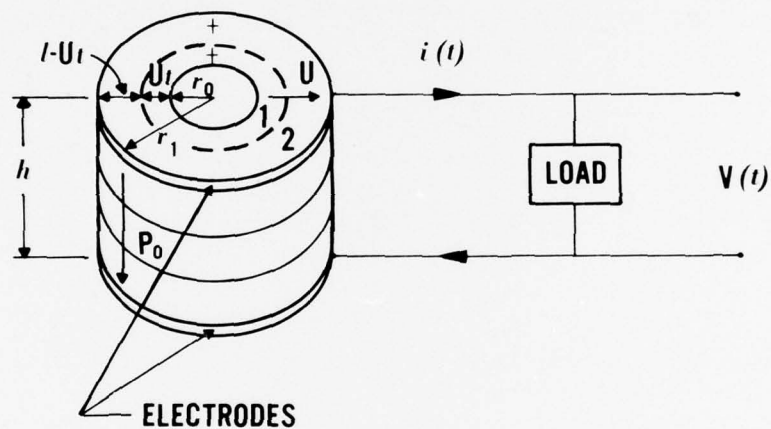
Figure 1. Schematic of the normal-mode depoling of (a) a rectangular PZT unit and (b) a hollow-cylinder PZT unit with an arbitrary load. A unit consists of a stack of PZT elements. The rectangular unit has width w, length ℓ, and height h. A shock wave enters the left surface of the unit and propagates in the direction ℓ with a steady shock velocity U. The hollow-cylinder unit has inner radius r_0, outer radius r_1, wall thickness ℓ, and height h. A shock wave enters the inner surface of the unit and propagates outward in a radial direction with a steady shock velocity U. At time t the shock front is indicated by the dashed lines. Regions 1 and 2 are behind and ahead of the shock front, respectively. It is assumed that the remanent polarization P_0 is reduced to zero by the propagating shock wave, thereby releasing the bound surface charge behind the shock front. The released charge is distributed between the PZT unit and the load, resulting in a voltage V(t).

3

and

$$C_2(t) = \frac{A\epsilon}{h}\left(1 - \frac{t}{\tau}\right), \quad 0 \leqslant t \leqslant \tau, \tag{3}$$

where ϵ is the constant permittivity of the PZT material. The equivalent capacitance of the PZT unit is constant and given by

$$C = C_1(t) + C_2(t) = \frac{A\epsilon}{h}, \quad t \geqslant 0. \tag{4}$$

For the hollow-cylinder PZT unit, the shock wave propagates outward in a radial direction. The released charge at time t is given by

$$q(t) = \begin{cases} P_0 A \dfrac{\left(\dfrac{2r_0}{\ell} + \dfrac{t}{\tau}\right)}{\left(\dfrac{2r_0}{\ell} + 1\right)}\left(\dfrac{t}{\tau}\right), & 0 \leqslant t \leqslant \tau, \\[1em] P_0 A, & t > \tau, \end{cases} \tag{5}$$

where $A = \pi\ell^2[(2r_0/\ell) + 1]$ and $\tau = \ell/U$. The PZT capacitances behind and ahead of the shock front are, respectively,

$$C_1(t) = \frac{A\epsilon}{h}\frac{\left(\dfrac{2r_0}{\ell} + \dfrac{t}{\tau}\right)}{\left(\dfrac{2r_0}{\ell} + 1\right)}\left(\frac{t}{\tau}\right), \quad 0 \leqslant t \leqslant \tau, \tag{6}$$

and

$$C_2(t) = \frac{A\epsilon}{h}\left[1 - \frac{\left(\dfrac{2r_0}{\ell} + \dfrac{t}{\tau}\right)}{\left(\dfrac{2r_0}{\ell} + 1\right)}\left(\frac{t}{\tau}\right)\right], \quad 0 \leqslant t \leqslant \tau. \tag{7}$$

4

The equivalent capacitance of the PZT unit is constant and given by

$$C = C_1(t) + C_2(t) = \frac{A\epsilon}{h} \ , \quad t \geqslant 0 \ . \tag{8}$$

The above expressions for the hollow-cylinder PZT unit reduce to those for the rectangular PZT unit for $r_0/\ell \gg 1$. In this case the geometrical factor $[(2r_0/\ell) + t/\tau]/[(2r_0/\ell) + 1]$ in Equations (5), (6), and (7) approaches a value of 1. The shock depoling of a thin-walled hollow-cylinder unit will give essentially the same time dependence of charge release as the shock depoling of a rectangular unit.

III. RESISTIVE LOAD

A. GENERAL CIRCUIT EQUATIONS

In this section, the load in Figures 1(a) and 1(b) is taken to be a resistance R. The voltage balance equation is

$$\frac{q_c(t)}{C} = i(t)R = V(t) \ , \quad t \geqslant 0 \ , \tag{9}$$

where $q_c(t)$ is the charge on the PZT unit at time t, and C is the capacitance of the unit which is given either by Equation (4) or (8). The charge conservation equation is

$$q(t) = q_c(t) + \int_0^t i(t)dt \ , \quad t \geqslant 0 \ . \tag{10}$$

Differentiating Equation (10) and substituting i(t) from Equation (9) gives

$$\frac{dq_c(t)}{dt} + \frac{q_c(t)}{RC} = \frac{dq(t)}{dt} \ , \quad t \geqslant 0 \ . \tag{11}$$

5

This equation can be solved for $q_c(t)$ by substituting $q(t)$ from either Equation (1) or (5). For $0 \leqslant t \leqslant \tau$, the initial condition $q_c(0) = 0$ is used for obtaining $q_c(t)$. For $t > \tau$, the derived expression for $q_c(\tau)$ is used as an initial condition.

B. RECTANGULAR PZT UNIT

In this section, expressions for the charge, voltage, current, and energy for the rectangular PZT unit with a resistive load are derived. The charge $q_c(t)$ is obtained by solving Equation (11) and using $q(t)$ from Equation (1). The result is

$$q_c(t) = \begin{cases} P_0 A \left(\dfrac{RC}{\tau} \right)(1 - e^{-t/RC}) & , \quad 0 \leqslant t \leqslant \tau, \\[4mm] P_0 A \left(\dfrac{RC}{\tau} \right)(e^{\tau/RC} - 1)e^{-t/RC} & , \quad t > \tau. \end{cases} \qquad (12)$$

The voltage on the PZT unit can be obtained from the expression

$$V(t) = \frac{q_c(t)}{C} \quad , \quad t \geqslant 0 . \qquad (13)$$

Figure 2(a) is a plot of the normalized charge and voltage for various values of RC/τ. The circuit current is obtained from the expression

$$i(t) = \frac{q_c(t)}{RC} \quad , \quad t \geqslant 0 . \qquad (14)$$

Figure 2(b) is a plot of the normalized current for various values of RC/τ. For a given shock transit time τ and PZT capacitance C, the magnitude of the corresponding resistive load R can be obtained for each curve in the figure. Current histories for normal-mode-depoled PZT 95/5 rectangular units have been measured as a function of load resistance.[3,11] (PZT 95/5 is a solid solution containing 95 mole % lead zirconate and 5 mole % lead titanate with niobium as a minor added constituent.) Although charge conduction occurred in the PZT material, the current histories are similar to those in Figure 2(b).

6

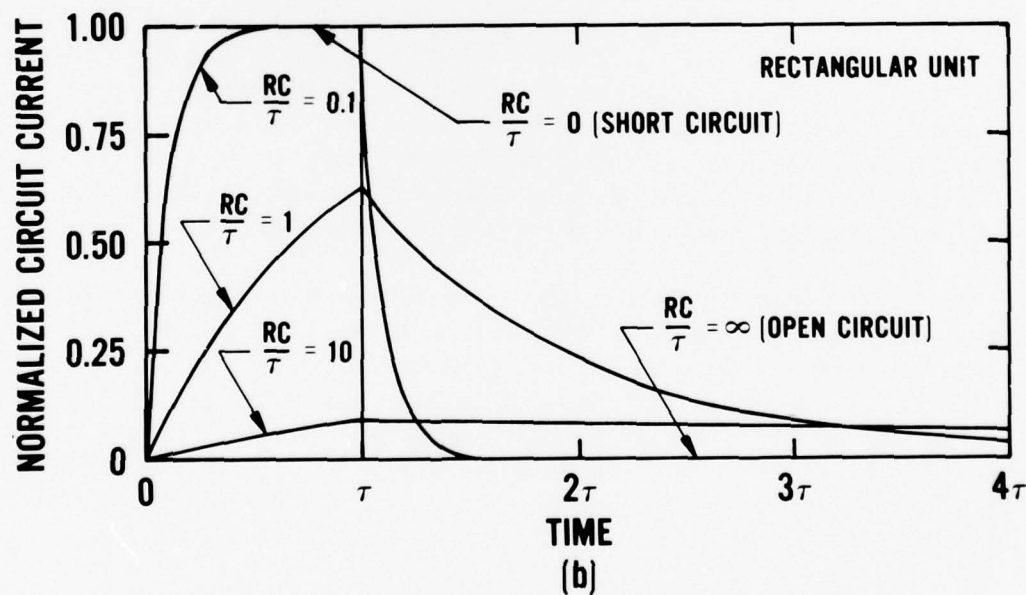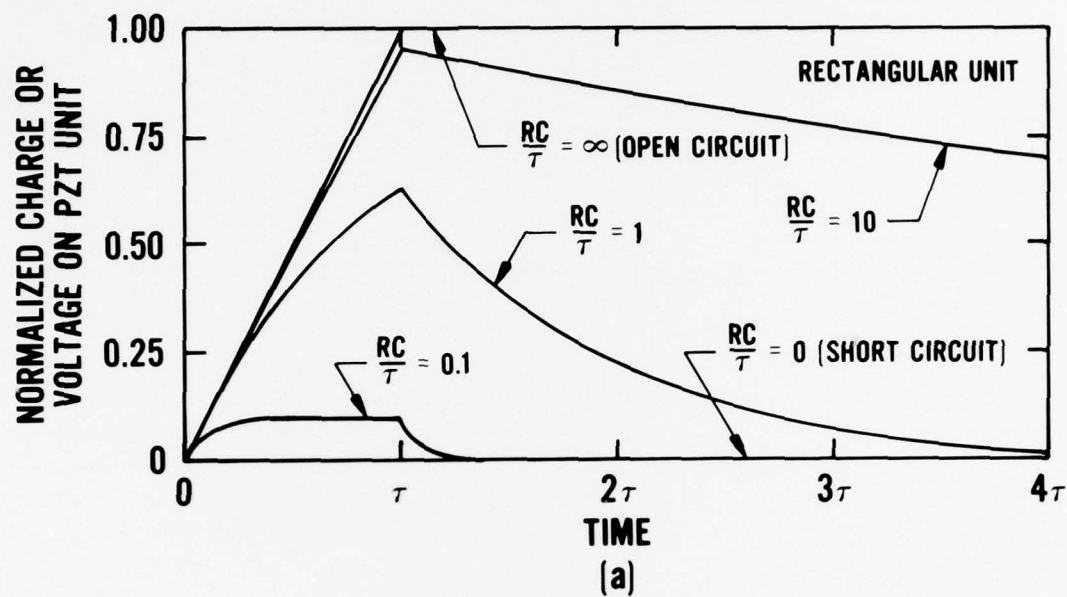Figure 2. Electrical relations for a rectangular PZT unit with a resistive load for various values of RC/τ. (a) Normalized charge $q_c(t)/P_0 A$ or voltage $V(t)/(P_0 A/C)$ on the PZT unit. (b) Normalized circuit current $i(t)/(P_0 A/\tau)$.

7

The amount of charge that has flowed through the resistance at time t is given by Equation (10). Making substitutions for q(t) and $q_c(t)$ gives for this charge

$$
\int_0^t i(t)dt = \begin{cases} P_0 A \left[\dfrac{t}{\tau} - \dfrac{RC}{\tau}(1 - e^{-t/RC}) \right], & 0 \leqslant t \leqslant \tau, \\[4mm] P_0 A \left[1 - \dfrac{RC}{\tau}(e^{\tau/RC} - 1)e^{-t/RC} \right], & t > \tau. \end{cases}
\tag{15}
$$

For the open-circuit case ($RC/\tau = \infty$), $q_c(t) = q(t)$. All the released charge remains on the PZT unit for all time t. For this case the charge and voltage on the PZT unit are linear functions of time for $0 \leqslant t \leqslant \tau$ and constant for $t > \tau$. The current is zero for all time t. Figure 2 shows these relationships. For the short-circuit case ($RC/\tau = 0$), $q_c(t) = 0$ for all t and $i(t) = P_0 A/\tau$ for $0 \leqslant t \leqslant \tau$ and equals zero for $t > \tau$. No charge remains on the PZT unit. All the charge is released in the time interval $0 \leqslant t \leqslant \tau$. For RC/τ between these two extremes, the PZT unit is charged during the interval $0 \leqslant t \leqslant \tau$ and discharged for $t > \tau$. As RC/τ increases from the short-circuit case, more charge remains on the PZT unit during the shock transit time. A maximum voltage of $P_0 A/C$ occurs at shock transit time for the open-circuit case. For a sufficiently large remanent polarization P_0, this maximum voltage can be large enough to cause electrical breakdown in the PZT unit. The area under the current pulse curves is given by $P_0 A$ for all values of RC/τ except ∞. This means that for large enough times, all the released charge flows through the resistance. For $RC/\tau = \infty$, no charge flows through the resistance.

It is not necessary to have exactly zero resistance R to observe the short-circuit current pulse in Figure 2(b). In some cases, an R of 100 Ω or even 1 kΩ will not affect (as observed experimentally) the amplitude of the short-circuit current pulse. It is only necessary that RC/τ be small enough that the shape of the measured pulse is essentially the same as the short-circuit case. For example, if C = 250 pF and τ = 2.5 μs (values from Reference 1) the ratio RC/τ is 0.01 for an R of 100 Ω. In Figure 2(b), the current pulse for this case would be essentially unchanged from the $RC/\tau = 0$ case.

From this discussion it can be concluded that the important circuit parameters are the shock transit time τ and the RC time constant. τ is the controlling parameter for small RC/τ; charge flows to the external circuit as fast as it is released by the shock wave. RC is the controlling parameter for large RC/τ; charge

8

is released to the PZT unit by the shock wave at a faster rate than it flows to the external circuit. Therefore, charge and voltage on the unit increase during shock transit time.

An interesting point to consider is an increase in the magnitude of the shock velocity. As the shock velocity U approaches infinity, the shock transit time τ approaches zero. This means that there is no charging phase for the PZT unit; i.e., at t = 0 the charge P_0A appears on the PZT unit. Expressions for the charge $q_c(t)$ and current i(t) for the discharging phase, t > 0, can be obtained from Equations (12) and (14), respectively, using the equations for t > τ.

For τ = 0, the charge becomes

$$q_c(t,\tau = 0) = \lim_{\tau \to 0}\left[P_0A\left(\frac{RC}{\tau}\right)(e^{\tau/RC} - 1)e^{-t/RC}\right] = P_0A\,e^{-t/RC}\,, \quad t > 0\,. \quad (16)$$

The current is given by

$$i(t,\tau = 0) = \frac{P_0A}{RC}\,e^{-t/RC}\,, \quad t > 0\,. \quad (17)$$

These equations are the expressions for discharging a capacitor with initial charge P_0A through a resistance R. For R = ∞, $q_c(t,\tau = 0) = P_0A$ and $i(t,\tau = 0) = 0$; i.e., the charge remains on the PZT unit. For R = 0, $q_c(t,\tau = 0) = 0$ and $i(t,\tau = 0) = \infty$. This case is analagous to short circuiting a charged capacitor.

An expression for the electrical energy dissipated in the resistance is given by

$$E_L(t) = R\int_0^t i^2(t)\,dt\,, \quad t \geqslant 0\,. \quad (18)$$

To solve this equation, use i(t) = $q_c(t)/RC$ and i(t)dt = dq - dq_c. Substituting gives

$$E_L(t) = \int_0^t \frac{q_c}{C}dq - \int_0^t \frac{q_c}{C}dq_c\,, \quad t \geqslant 0\,. \quad (19)$$

9

Integrating the last term and using $E_T(t) = E_C(t) + E_L(t)$ and

$$E_C(t) = \frac{q_c^2(t)}{2C} , \quad t \geq 0, \tag{20}$$

gives

$$E_T(t) = \int_0^t \frac{q_c dq}{C} , \quad t \geq 0 . \tag{21}$$

This is the electrical energy equation for the circuit. The electrical energy in the circuit increases for $0 \leq t \leq \tau$ to a maximum value determined by the integral in the above equation. For $t > \tau$ the energy does not increase because $dq = 0$. Evaluating the integral gives

$$E_T(t) = \begin{cases} \dfrac{P_0 A}{C} \left(\dfrac{RC}{\tau}\right) [q(t) - q_c(t)] , & 0 \leq t \leq \tau , \\[2mm] \dfrac{P_0 A}{C} \left(\dfrac{RC}{\tau}\right) [q(\tau) - q_c(\tau)] , & t > \tau . \end{cases} \tag{22}$$

Figures 3(a), 3(b), and 3(c) are, respectively, the normalized energy on the PZT unit obtained from Equation (20), the normalized energy dissipated in the resistance obtained from Equation (18), and the total normalized circuit energy obtained from Equation (22).

For the short-circuit case ($RC/\tau = 0$), $E_T(t) = 0$ for all t. All released charge flows immediately in the external circuit. $E_C(t) = 0$, because there is no charge or voltage buildup on the PZT unit and $E_L(t) = 0$ because the resistance is zero. This corresponds to the case of current flowing (magnitude $P_0 A/\tau$), but no electrical energy is being stored or dissipated.

Maximum electrical energy is stored on the PZT unit for the open-circuit case ($RC/\tau = \infty$). Also, $E_L(t) \approx 0$ for all t because all the charge is stored on the capacitance. As $RC/\tau \to \infty$, Equation (22) becomes

$$E_T(t, RC/\tau = \infty) = \begin{cases} \dfrac{(P_0 A)^2}{2C} \left(\dfrac{t}{\tau}\right)^2 , & 0 \leq t \leq \tau , \\[2mm] \dfrac{(P_0 A)^2}{2C} , & t > \tau . \end{cases} \tag{23}$$
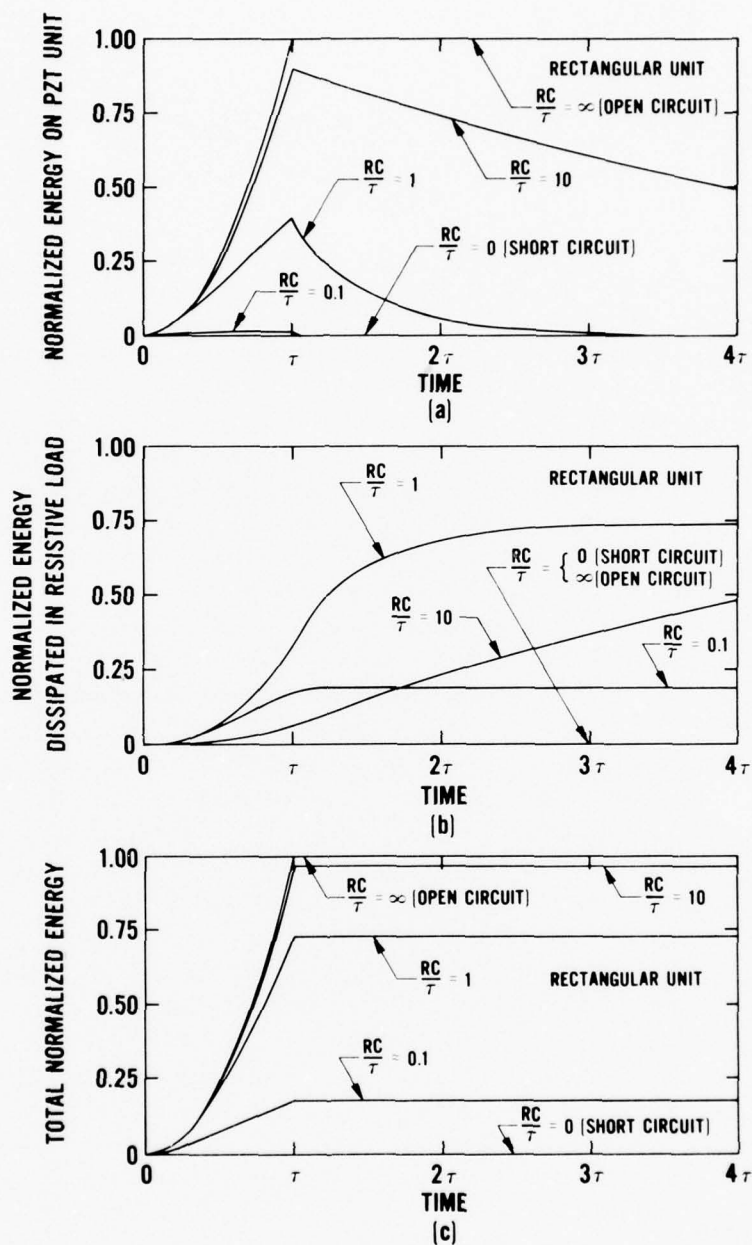
10

Figure 3. Energy relations for a rectangular PZT unit with a resistive load for various values of RC/τ. (a) Normalized energy $E_C(t)/((P_0A)^2/2C)$ on the PZT unit. (b) Normalized energy $E_L(t)/((P_0A)^2/2C)$ dissipated in the resistive load. (c) Total normalized energy $E_T(t)/((P_0A)^2/2C)$.

11

This can be shown by using

$$q(t) - q_c(t) = \frac{P_0 A}{2} \left(\frac{\tau}{RC}\right) \left(\frac{t}{\tau}\right)^2 + \text{higher order} \left(\frac{t}{RC}\right) \text{ terms}, \quad 0 \leqslant t \leqslant \tau, \quad (24)$$

as $RC/\tau \to \infty$.

The expression $(P_0 A)^2/2C$ is the maximum energy for an ideal PZT unit. This energy is usually not achieved in a depoling experiment for a PZT unit poled to maximum remanent polarization, since the associated voltage $P_0 A/C$ gives an electric field that can be much larger than the breakdown strength of the PZT material. For example, in Reference 1, some of the PZT 56/44 units that were shock loaded were cubes with a side d of 12.7 mm. The units had a polarization P_0 of 0.33 $\mu C/mm^2$, an available charge $P_0 A$ of 50 μC, and a capacitance C of about 250 pF. (PZT 56/44 is a solid solution containg 56 mole % lead zirconate and 44 mole % lead titanate with minor added constituents of niobium, strontium, and lanthanum.) For these units the calculated voltage $P_0 A/C$ is 200 kV and the calculated electric field $(P_0 A/C)/d$ is 15.7 kV/mm. This electric field is about four times larger than a breakdown field of 3.7 kV/mm for a similar material, PZT 65/35, measured under ambient conditions.[1,2] (PZT 65/35 is a solid solution containing 65 mole % lead zirconate and 35 mole % lead titanate with niobium as a minor added constituent.) To prevent electrical breakdown, it becomes necessary to choose the load parameters so that the circuit voltage and the corresponding electric field are reduced. Therefore, only a fraction of the energy $(P_0 A)^2/2C$ and energy density $((P_0 A)^2/2C)/d^3$ of 5 J and 2.5 J/cm^3, respectively, are available from the PZT unit. It should be noted that if the PZT 56/44 material were poled to a remanent polarization value less than the representative value of 0.33 $\mu C/mm^2$, then electrical breakdown in the unit would be less likely to occur and the energy $(P_0 A)^2/2C$ would then be achieved at a lower but more realistic value.

Figure 3 indicates that electrical energy is both supplied to the PZT unit and dissipated in the resistance during shock transit time τ. But for $t > \tau$ the total circuit energy is constant; energy on the PZT unit is being dissipated in the resistance. For example, at $t = \tau$ for the $RC/\tau = 1$ curves, the normalized circuit energy is about 73%. About 40% is stored on the PZT unit and about 33% has been dissipated in the resistance. For $t > \tau$ the 40% stored on the unit is dissipated in about 2τ. Figure 4 is a set of normalized energy curves showing this behavior at $t = \tau$ for RC/τ ranging from 10^{-3} to 10^3. The curve for the energy dissipated in the resistance reaches a maximum for $RC/\tau = 0.529$. The maximum energy dissipated is $0.381((P_0 A)^2/2C)$. This can be contrasted with the maximum voltage which occurs for $RC/\tau = \infty$ and the maximum charge transfer which occurs

12

for $RC/\tau = 0$. At maximum energy transfer the energy on the PZT unit is about $0.2((P_0 A)^2/2C)$. Also, the energy stored on the PZT unit equals the energy dissipated in the resistance for $RC/\tau = 0.868$.

C. HOLLOW-CYLINDER PZT UNIT

In this section expressions are derived for the charge, voltage, current, and energy in a circuit consisting of a hollow-cylinder PZT unit with a resistive load. Due to the cylindrical geometry, the expressions are more complicated than those derived in the last section for the rectangular unit. The charge $q_c(t)$ on the PZT unit is obtained by solving Equation (11) with $q(t)$ from Equation (5). This gives

$$q_c(t) = \begin{cases} P_0 A \left(\dfrac{RC}{\tau}\right) \dfrac{\left(\dfrac{2r_0}{\ell} - \dfrac{2RC}{\tau}\right)}{\left(\dfrac{2r_0}{\ell} + 1\right)} \left[(1 - e^{-t/RC}) + \dfrac{\dfrac{2t}{\tau}}{\left(\dfrac{2r_0}{\ell} - \dfrac{2RC}{\tau}\right)}\right], & 0 \leqslant t \leqslant \tau, \\[30pt] P_0 A \left(\dfrac{RC}{\tau}\right) \dfrac{\left(\dfrac{2r_0}{\ell} - \dfrac{2RC}{\tau}\right)}{\left(\dfrac{2r_0}{\ell} + 1\right)} \left[(e^{\tau/RC} - 1)e^{-t/RC} + \dfrac{2e^{-(t-\tau)/RC}}{\left(\dfrac{2r_0}{\ell} - \dfrac{2RC}{\tau}\right)}\right], & t > \tau. \end{cases} \qquad (25)$$

This equation can be compared with Equation (12) for the rectangular PZT unit. For the open-circuit case ($RC/\tau = \infty$), Equation (25) reduces to

$$q_c(t, RC/\tau = \infty) = \begin{cases} P_0 A \dfrac{\left(\dfrac{2r_0}{\ell} + \dfrac{t}{\tau}\right)}{\left(\dfrac{2r_0}{\ell} + 1\right)} \left(\dfrac{t}{\tau}\right), & 0 \leqslant t \leqslant \tau, \\[20pt] P_0 A, & t > \tau. \end{cases} \qquad (26)$$

This is just Equation (5) for the charge release $q(t)$.

Equations for the voltage $V(t)$ on the hollow-cylinder PZT unit and current $i(t)$ in the circuit can be obtained by substituting Equation (25) for $q_c(t)$ into Equations (13) and (14), respectively. Figure 5(a) is a plot of the normalized charge

13
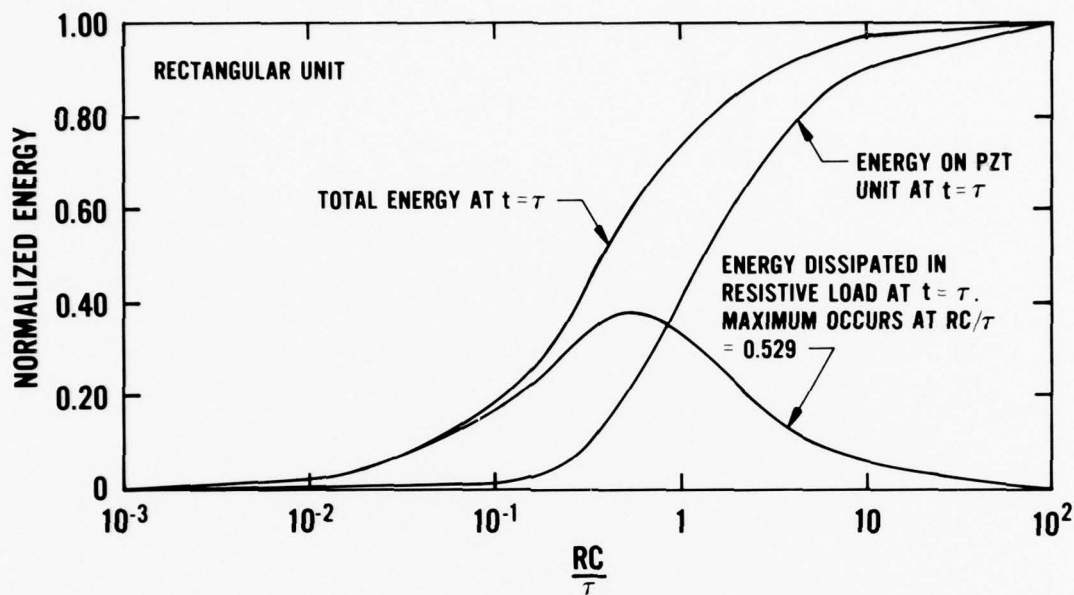
Figure 4. Normalized energy relations for a rectangular PZT unit with a resistive load at shock transit time τ as a function of RC/τ.

and voltage on the PZT unit for a representative r_0/ℓ value of 1. The time dependences for the cylindrical and rectangular geometries are the same for $t > \tau$. This is expected since after the shock wave passes out of the unit, the charge remaining on the unit in both cases decays with the RC time constant. Notice also that the curves in Figure 5(a) are similar to those in Figure 2(a) for the rectangular unit. In addition, it can be shown that Equation (25) reduces to Equation (12) for $r_0/\ell \gg 1$. This can be shown using $[(2r_0/\ell) - 2RC/\tau]/[(2r_0/\ell) + 1] \rightarrow 1$ and $1/[(2r_0/\ell) - 2RC/\tau] \rightarrow 0$ as $r_0/\ell \rightarrow \infty$.

Figure 5(b) is a plot of the normalized current. For $0 \leqslant t \leqslant \tau$ the short-circuit current increases linearly with time. This increase becomes less as r_0/ℓ becomes larger and, as expected, approaches the case for the rectangular unit as $r_0/\ell \rightarrow \infty$. The short-circuit current is

14
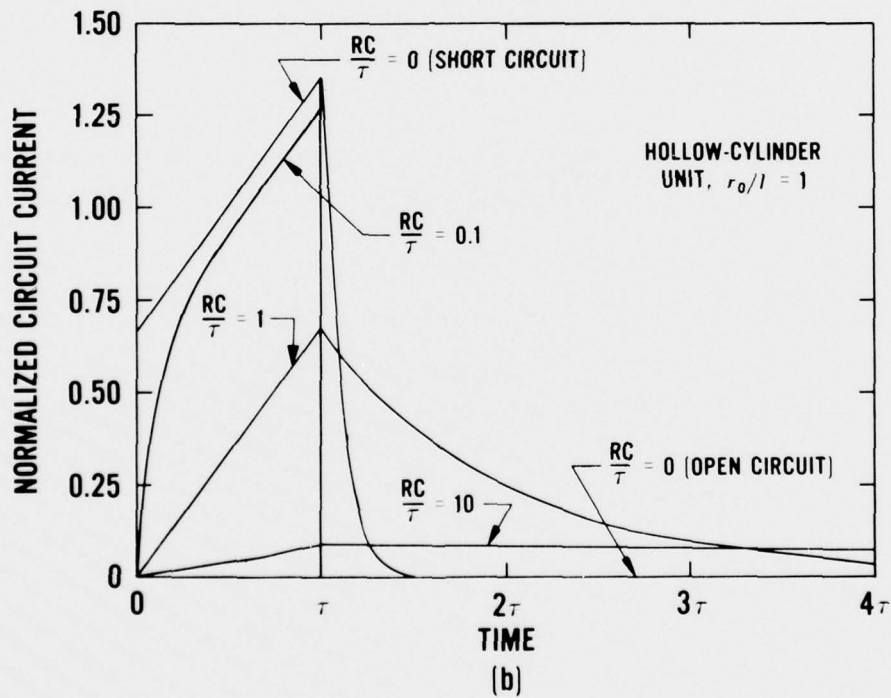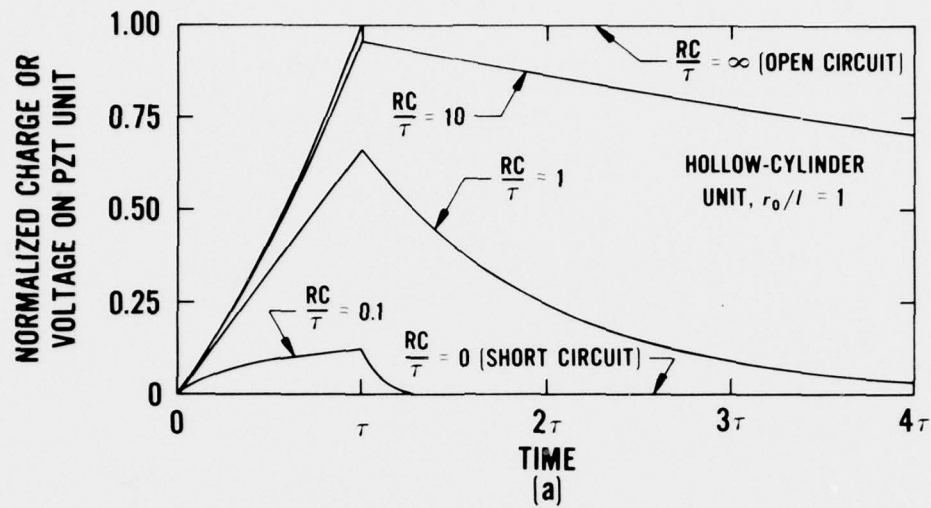
Figure 5. Electrical relations for a hollow-cylinder PZT unit with a resistive load for various values of RC/τ. Curves are given for $r_0/\ell = 1$. (a) Normalized charge $q_c(t)/P_0 A$ or voltage $V(t)/(P_0 A/C)$ on the PZT unit. (b) Normalized circuit current $i(t)/(P_0 A/\tau)$.

15

$$i(t, RC/\tau = 0) = \begin{cases} \dfrac{P_0 A}{\tau} \dfrac{\left(\dfrac{2r_0}{\ell} + \dfrac{2t}{\tau}\right)}{\left(\dfrac{2r_0}{\ell} + 1\right)}, & 0 \leqslant t \leqslant \tau, \\[4mm] 0, & t > \tau. \end{cases} \tag{27}$$

At $t = \tau/2$, $i(\tau/2, RC/\tau = 0) = P_0 A/\tau$ as shown in Figure 5(b). The integral of the short-circuit current is

$$\int_0^\tau i(t, RC/\tau = 0) dt = P_0 A \tag{28}$$

as expected.

The total circuit energy can be derived from Equation (21) by substituting $q(t)$ from Equation (5) and $q_c(t)$ from Equation (25) and integrating. The result is

$$E_T(t) = \begin{cases} \dfrac{P_0 A}{C} \left(\dfrac{RC}{\tau}\right) \dfrac{\left(\dfrac{2r_0}{\ell} + \dfrac{2RC}{\tau}\right)}{\left(\dfrac{2r_0}{\ell} + 1\right)} \left[[q(t) - q_c(t)] - \dfrac{\dfrac{2t}{\tau} q_c(t)}{\left(\dfrac{2r_0}{\ell} + \dfrac{2RC}{\tau}\right)} + 4P_0 A \dfrac{\left(\dfrac{r_0}{2\ell} + \dfrac{t}{3\tau}\right)}{\left(\dfrac{2r_0}{\ell} + 1\right)\left(\dfrac{2r_0}{\ell} + \dfrac{2RC}{\tau}\right)} \left(\dfrac{t}{\tau}\right)^2 \right], & 0 \leqslant t \leqslant \tau, \\[8mm] \dfrac{P_0 A}{C} \left(\dfrac{RC}{\tau}\right) \dfrac{\left(\dfrac{2r_0}{\ell} + \dfrac{2RC}{\tau}\right)}{\left(\dfrac{2r_0}{\ell} + 1\right)} \left[[q(\tau) - q_c(\tau)] - \dfrac{2q_c(\tau)}{\left(\dfrac{2r_0}{\ell} + \dfrac{2RC}{\tau}\right)} + 4P_0 A \dfrac{\left(\dfrac{r_0}{2\ell} + \dfrac{1}{3}\right)}{\left(\dfrac{2r_0}{\ell} + 1\right)\left(\dfrac{2r_0}{\ell} + \dfrac{2RC}{\tau}\right)} \right], & t > \tau. \end{cases} \tag{29}$$

16

It can be seen that as $r_0/\ell \to \infty$ this equation reduces to Equation (22) for the rectangular unit. For the open-circuit case ($RC/\tau = \infty$), Equation (29) reduces to

$$
E_T(t) = \begin{cases}
\dfrac{(P_0 A)^2}{2C} \ \dfrac{\left(\dfrac{2r_0}{\ell} + \dfrac{t}{\tau}\right)^2}{\left(\dfrac{2r_0}{\ell} + 1\right)^2} \left(\dfrac{t}{\tau}\right)^2 \ , & 0 \leqslant t \leqslant \tau, \\[2em]
\dfrac{(P_0 A)^2}{2C} & , \qquad t > \tau.
\end{cases}
\tag{30}
$$

To show this, it is necessary to expand $q_c(t)$ in Equation (25) for $RC/\tau \to \infty$ and then form the expansion $q(t) - q_c(t)$. The expansions for $0 \leqslant t \leqslant \tau$ are

$$
q_c(t) = \frac{P_0 A}{\left(\dfrac{2r_0}{\ell} + 1\right)} \left[\left(\frac{2r_0}{\ell} + \frac{t}{\tau}\right)\frac{t}{\tau} - \left(\frac{r_0}{\ell} + \frac{t}{3\tau}\right)\frac{t^2}{RC\tau} + \left(\frac{r_0}{3\ell} + \frac{t}{12\tau}\right)\frac{t^3}{(RC)^2\tau} - \cdots \right], \quad 0 \leqslant t \leqslant \tau,
\tag{31}
$$

and

$$
q(t) - q_c(t) = \frac{P_0 A}{\left(\dfrac{2r_0}{\ell} + 1\right)} \left[\left(\frac{r_0}{\ell} + \frac{t}{3\tau}\right)\frac{t^2}{RC\tau} - \left(\frac{r_0}{3\ell} + \frac{t}{12\tau}\right)\frac{t^3}{(RC)^2\tau} + \cdots \right], \quad 0 \leqslant t \leqslant \tau.
\tag{32}
$$

Figures 6(a), 6(b), and 6(c) are, respectively, plots of the normalized PZT energy, normalized energy dissipated in the resistive load, and total normalized energy. Figure 7 gives the normalized energy relations for the hollow-cylinder unit. Plots of total energy, capacitive energy, and resistive energy are given at $t = \tau$. The resistive energy peaks around $RC/\tau = 0.5$. These curves are similar to the curves in Figure 4 for the rectangular PZT unit.

17

It can be seen that as $r_0/\ell \to \infty$ this equation reduces to Equation (22) for the rectangular unit. For the open-circuit case ($RC/\tau = \infty$), Equation (29) reduces to

$$
E_T(t) = \begin{cases} \dfrac{(P_0 A)^2}{2C} \dfrac{\left(\dfrac{2r_0}{\ell} + \dfrac{t}{\tau}\right)^2}{\left(\dfrac{2r_0}{\ell} + 1\right)^2} \left(\dfrac{t}{\tau}\right)^2 , & 0 \leqslant t \leqslant \tau, \\[4ex] \dfrac{(P_0 A)^2}{2C} & , \qquad t > \tau . \end{cases}
\tag{30}
$$

To show this, it is necessary to expand $q_c(t)$ in Equation (25) for $RC/\tau \to \infty$ and then form the expansion $q(t) - q_c(t)$. The expansions for $0 \leqslant t \leqslant \tau$ are

$$
q_c(t) = \frac{P_0 A}{\left(\dfrac{2r_0}{\ell} + 1\right)} \left[\left(\frac{2r_0}{\ell} + \frac{t}{\tau}\right) \frac{t}{\tau} - \left(\frac{r_0}{\ell} + \frac{t}{3\tau}\right) \frac{t^2}{RC\tau} + \left(\frac{r_0}{3\ell} + \frac{t}{12\tau}\right) \frac{t^3}{(RC)^2 \tau} - \cdots \right], \quad 0 \leqslant t \leqslant \tau,
\tag{31}
$$

and

$$
q(t) - q_c(t) = \frac{P_0 A}{\left(\dfrac{2r_0}{\ell} + 1\right)} \left[\left(\frac{r_0}{\ell} + \frac{t}{3\tau}\right) \frac{t^2}{RC\tau} - \left(\frac{r_0}{3\ell} + \frac{t}{12\tau}\right) \frac{t^3}{(RC)^2 \tau} + \cdots \right], \quad 0 \leqslant t \leqslant \tau .
\tag{32}
$$

Figures 6(a), 6(b), and 6(c) are, respectively, plots of the normalized PZT energy, normalized energy dissipated in the resistive load, and total normalized energy. Figure 7 gives the normalized energy relations for the hollow-cylinder unit. Plots of total energy, capacitive energy, and resistive energy are given at $t = \tau$. The resistive energy peaks around $RC/\tau = 0.5$. These curves are similar to the curves in Figure 4 for the rectangular PZT unit.

Figure 6. Energy relations for a hollow-cylinder PZT unit with a resistive load for various values of RC/τ. Curves are given for $r_0/\ell = 1$. (a) Normalized energy $E_C(t)/((P_0 A)^2/2C)$ on the PZT unit. (b) Normalized energy $E_L(t)/((P_0 A)^2/2C)$ dissipated in the resistive load. (c) Total normalized energy $E_T(t)/((P_0 A)^2/2C)$.

18
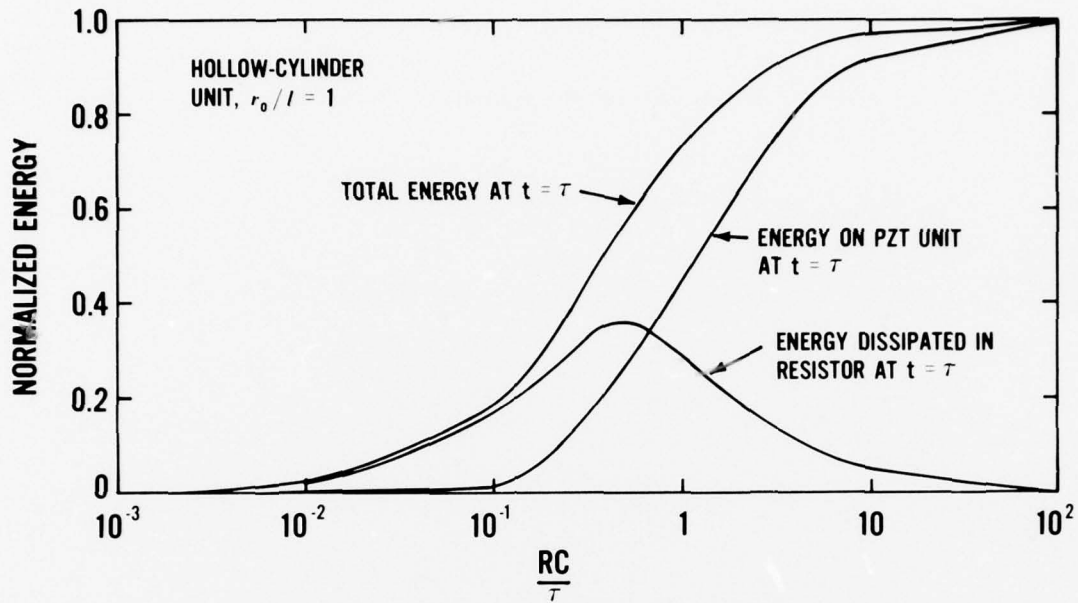
Figure 7. Normalized energy relations for a hollow-cylinder PZT unit with a resistive load at shock transit time τ as a function of RC/τ. Curves are given for $r_0/\ell = 1$.

IV. CAPACITIVE LOAD

A. GENERAL CIRCUIT EQUATIONS

In this section, the load in Figures 1(a) and 1(b) is a capacitance C_L. The voltage balance equation is

$$\frac{q_C(t)}{C} = \frac{q_L(t)}{C_L}, \quad t \geq 0, \tag{33}$$

where C is the capacitance of the PZT unit given by either Equation (4) or (8). $q_C(t)$ is the charge on the PZT unit and $q_L(t)$ is the charge on the load capacitor. The charge conservation equation is

19

$$q(t) = q_C(t) + q_L(t) \quad , \quad t \geqslant 0 , \tag{34}$$

where $q(t)$ is the charge released by the shock wave. Solving these equations gives

$$q_C(t) = \frac{C}{C + C_L} \, q(t) \quad , \quad t \geqslant 0 , \tag{35}$$

and

$$q_L(t) = \frac{C_L}{C + C_L} \, q(t) \quad , \quad t \geqslant 0 . \tag{36}$$

The voltage on the PZT unit and load, and the current in the circuit are, respectively,

$$V(t) = \frac{q(t)}{C + C_L} \quad , \quad t \geqslant 0 , \tag{37}$$

and

$$i(t) = \frac{dq_L(t)}{dt} = \frac{C_L}{C + C_L} \frac{dq(t)}{dt} \quad , \quad t \geqslant 0 . \tag{38}$$

Equations (35) through (38) can be solved for the rectangular or hollow-cylinder unit by substituting $q(t)$ from Equations (1) or (5), respectively.

B. RECTANGULAR PZT UNIT

Using $q(t)$ from Equation (1) in Equations (35) through (37) gives

20

$$q_C(t) = \begin{cases} P_0 A \, \dfrac{C}{C+C_L} \left(\dfrac{t}{\tau}\right), & 0 \leqslant t \leqslant \tau, \\[3ex] P_0 A \, \dfrac{C}{C+C_L} & , \qquad t > \tau. \end{cases} \qquad (39)$$

$$q_L(t) = \begin{cases} P_0 A \, \dfrac{C_L}{C+C_L} \left(\dfrac{t}{\tau}\right), & 0 \leqslant t \leqslant \tau, \\[3ex] P_0 A \, \dfrac{C_L}{C+C_L} & , \qquad t > \tau. \end{cases} \qquad (40)$$

and

$$V(t) = \begin{cases} \dfrac{P_0 A}{C+C_L} \left(\dfrac{t}{\tau}\right), & 0 \leqslant t \leqslant \tau, \\[3ex] \dfrac{P_0 A}{C+C_L} & , \qquad t > \tau. \end{cases} \qquad (41)$$

Figure 8(a) is a plot of the normalized charge or voltage on the PZT unit. The charging region $(0 \leqslant t \leqslant \tau)$ is characterized by a constant slope determined by C_L/C. For the open-circuit case $(C_L/C = 0)$, no charge is transferred to the load; this is identical to the resistive case for $RC/\tau = \infty$ as shown in Figure 2(a). For the short-circuit case $(C_L/C = \infty)$, all the charge is transferred to the load capacitance at zero voltage; this situation is again identical to the resistive case for $RC/\tau = 0$.

The circuit current, obtained from Equation (38), is

$$i(t) = \begin{cases} \dfrac{P_0 A}{\tau} \, \dfrac{C_L}{C+C_L} & , \quad 0 \leqslant t \leqslant \tau, \\[3ex] 0 & , \qquad t > \tau. \end{cases} \qquad (42)$$

Figure 8. Electrical relations for a rectangular PZT unit with a capacitive load for various values of C_L/C. (a) Normalized charge $q_c(t)/P_0 A$ or voltage $V(t)/(P_0 A/C)$ on the PZT unit. (b) Normalized circuit current $i(t)/(P_0 A/\tau)$.

22

Figure 8(b) is a plot of the normalized current for the rectangular PZT unit. The current is a flat-topped pulse for $0 \leq t \leq \tau$ and zero for $t > \tau$. For the short-circuit case, the rate of charge release by the shock wave, $P_0 A/\tau$, equals the amplitude of the short-circuit current pulse. Equation (42) and Figure 8(b) show that the amplitude of the current pulse decreases as the C_L/C ratio decreases until, for the open-circuit case, the current is zero.

In recent experiments, rectangular PZT 56/44 and PZT 95/5 units were depoled in the normal mode with a capacitive load.[1] It was shown that for some stress values for each material the measured voltage and current pulses were similar to those in Figure (8).

The energy on the PZT unit is given by

$$
E_C(t) = \begin{cases} \dfrac{(P_0 A)^2}{2C} \left(\dfrac{C}{C + C_L}\right)^2 \left(\dfrac{t}{\tau}\right)^2 , & 0 \leq t \leq \tau , \\[4mm] \dfrac{(P_0 A)^2}{2C} \left(\dfrac{C}{C + C_L}\right)^2 , & t > \tau , \end{cases}
\tag{43}
$$

and the energy on the capacitive load is

$$
E_L(t) = \begin{cases} \dfrac{(P_0 A)^2}{2C} \dfrac{CC_L}{(C + C_L)^2} \left(\dfrac{t}{\tau}\right)^2 , & 0 \leq t \leq \tau , \\[4mm] \dfrac{(P_0 A)^2}{2C} \dfrac{CC_L}{(C + C_L)^2} , & t > \tau . \end{cases}
\tag{44}
$$

The total circuit energy $E_T(t) = E_C(t) + E_L(t)$ is

$$
E_T(t) = \begin{cases} \dfrac{(P_0 A)^2}{2C} \left(\dfrac{C}{C + C_L}\right) \left(\dfrac{t}{\tau}\right)^2 , & 0 \leq t \leq \tau , \\[4mm] \dfrac{(P_0 A)^2}{2C} \left(\dfrac{C}{C + C_L}\right) , & t > \tau . \end{cases}
\tag{45}
$$

23

Figures 9(a), 9(b), and 9(c) are, respectively, the normalized energy on the PZT unit, normalized energy on the load capacitance, and the total normalized energy. For the open-circuit case, all the released charge remains on the PZT unit; the circuit energy has a maximum value of $(P_0A)^2/2C$. For the short-circuit case all the energy equations are zero even though a current P_0A/τ flows in the circuit. This is analogous to the resistive load for $RC/\tau = 0$. As shown in Figure 9(b), the energy transferred to the load capacitance is a maximum for $C_L/C = 1$; this maximum value is $(P_0A)^2/8C$. In summary, the maximum charge is transferred to the load for $C_L/C = \infty$, but the maximum energy transfer occurs for $C_L/C = 1$.

C. HOLLOW-CYLINDER PZT UNIT

In this section, expressions are derived for the charge, voltage, current, and energy in a circuit consisting of a hollow-cylinder PZT unit and a capacitive load. The charge $q_C(t)$ on the PZT unit and $q_L(t)$ on the load capacitance are obtained by substituting $q(t)$ from Equation (5) into Equations (35) and (36), respectively. The result is

$$q_C(t) = \begin{cases} P_0A\,\dfrac{C}{C+C_L}\,\dfrac{\left(\dfrac{2r_0}{\ell}+\dfrac{t}{\tau}\right)}{\left(\dfrac{2r_0}{\ell}+1\right)}\left(\dfrac{t}{\tau}\right), & 0 \leqslant t \leqslant \tau, \\[2em] P_0A\,\dfrac{C}{C+C_L}, & t > \tau. \end{cases} \tag{46}$$

$$q_L(t) = \begin{cases} P_0A\,\dfrac{C_L}{C+C_L}\,\dfrac{\left(\dfrac{2r_0}{\ell}+\dfrac{t}{\tau}\right)}{\left(\dfrac{2r_0}{\ell}+1\right)}\left(\dfrac{t}{\tau}\right), & 0 \leqslant t \leqslant \tau, \\[2em] P_0A\,\dfrac{C_L}{C+C_L}, & t > \tau. \end{cases} \tag{47}$$
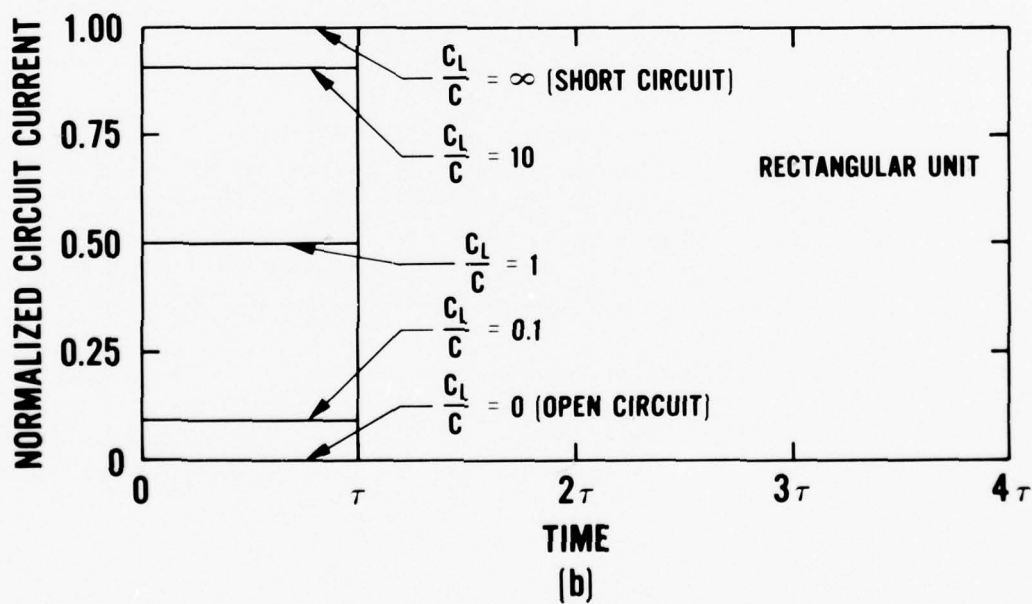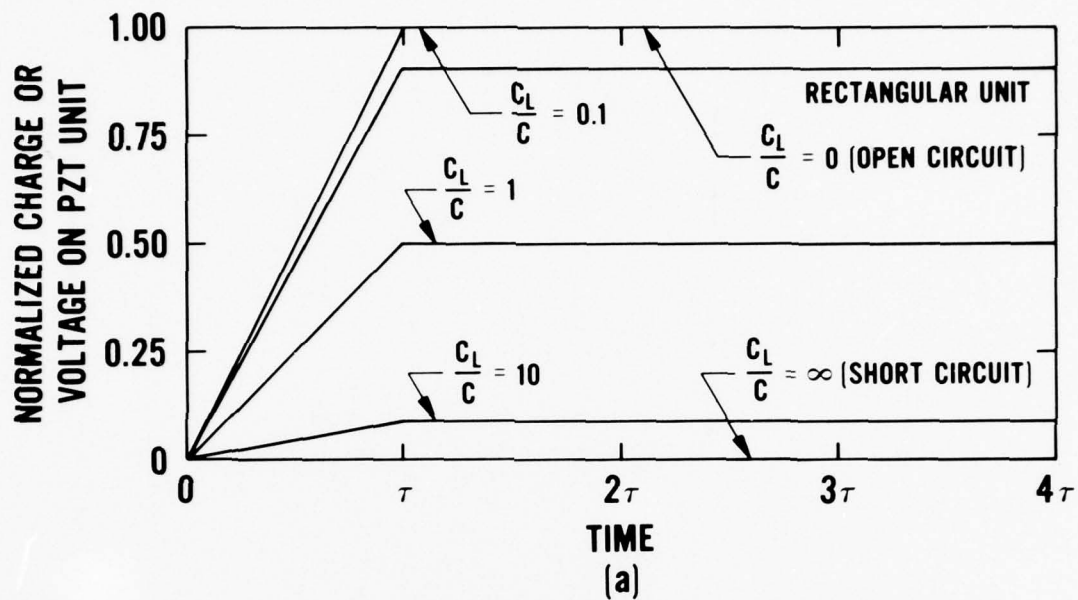
24
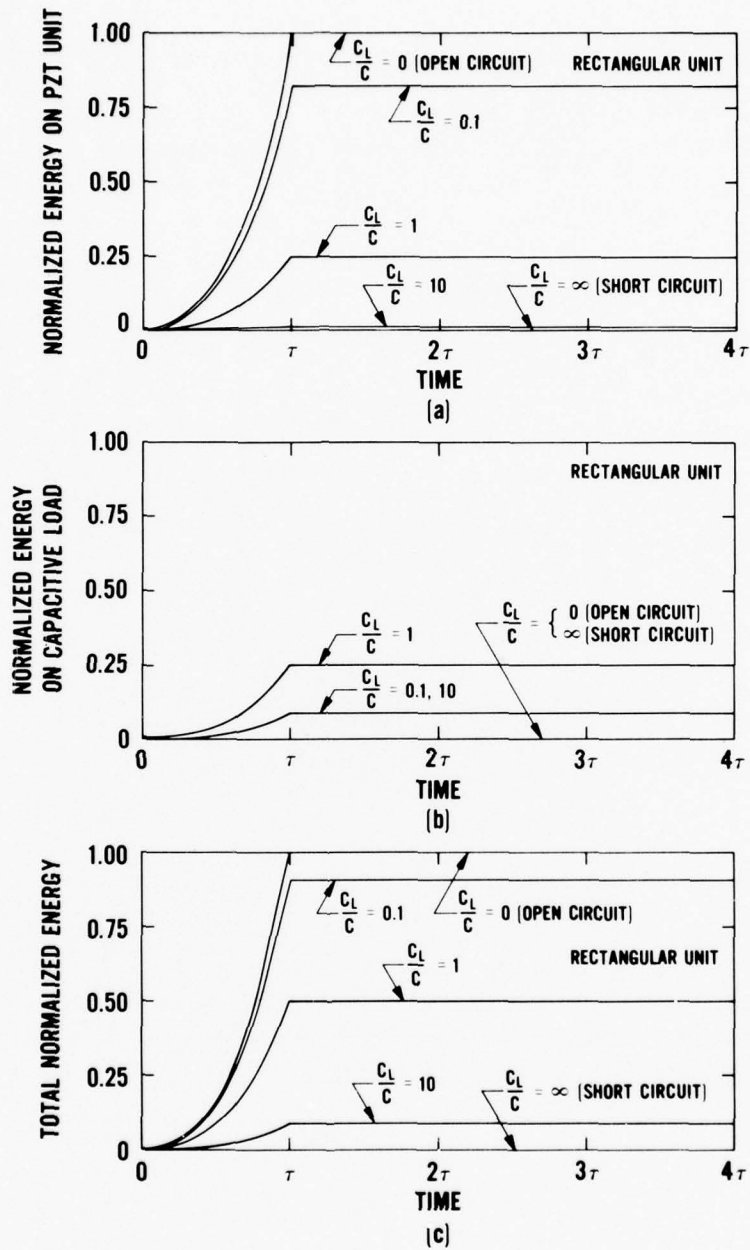
Figure 9. Energy relations for a rectangular PZT unit with a capacitive load for various values of C_L/C. (a) Normalized energy $E_C(t)/((P_0A)^2/2C)$ on the PZT unit. (b) Normalized energy $E_L(t)/((P_0A)^2/2C)$ on the capacitive load. (c) Total normalized energy $E_T(t)/((P_0A)^2/2C)$.

Using Equation (37), the voltage on the PZT unit and load capacitance is

$$
V(t) = \begin{cases} \dfrac{P_0 A}{C + C_L} \dfrac{\left(\dfrac{2r_0}{\ell} + \dfrac{t}{\tau}\right)}{\left(\dfrac{2r_0}{\ell} + 1\right)} \left(\dfrac{t}{\tau}\right) , & 0 \leqslant t \leqslant \tau , \\[20pt] \dfrac{P_0 A}{C + C_L} , & t > \tau . \end{cases}
\tag{48}
$$

Figure 10(a) is a plot of the normalized charge and voltage for $r_0/\ell = 1$. In the charging region ($0 \leqslant t \leqslant \tau$), the only difference between these curves and those for the rectangular unit in Figure 8(a) is the geometrical factor $[(2r_0/\ell) + (t/\tau)]/[(2r_0/\ell) + 1]$. As $r_0/\ell \to \infty$, the factor becomes 1 and the curves become identical. For the region $t > \tau$, the curves for the two geometries are the same.

The current equation is

$$
i(t) = \begin{cases} \dfrac{P_0 A}{\tau} \left(\dfrac{C_L}{C + C_L}\right) \dfrac{\left(\dfrac{2r_0}{\ell} + \dfrac{2t}{\tau}\right)}{\left(\dfrac{2r_0}{\ell} + 1\right)} , & 0 \leqslant t \leqslant \tau , \\[20pt] 0 , & t > \tau . \end{cases}
\tag{49}
$$

Figure 10(b) is a plot of the normalized current for $r_0/\ell = 1$. Again, these curves become identical to those for the rectangular unit in Figure 8(b) as $r_0/\ell \to \infty$. At $t/\tau = 0.5$, the normalized current for the hollow-cylinder and rectangular units are equal for any value of r_0/ℓ since for this case the geometrical factor is 1.

The energy on the PZT unit and load capacitance are given by

$$
E_C(t) = \begin{cases} \dfrac{(P_0 A)^2}{2C} \left(\dfrac{C}{C + C_L}\right)^2 \dfrac{\left(\dfrac{2r_0}{\ell} + \dfrac{t}{\tau}\right)^2}{\left(\dfrac{2r_0}{\ell} + 1\right)^2} \left(\dfrac{t}{\tau}\right)^2 , & 0 \leqslant t \leqslant \tau , \\[20pt] \dfrac{(P_0 A)^2}{2C} \left(\dfrac{C}{C + C_L}\right)^2 , & t > \tau . \end{cases}
\tag{50}
$$

26

Figure 10. Electrical relations for a hollow-cylinder PZT unit with a capacitive load for various values of C_L/C. Curves are given for $r_0/\ell = 1$. (a) Normalized charge $q_c(t)/P_0 A$ or voltage $V(t)/(P_0 A/C)$ on the PZT unit. (b) Normalized circuit current $i(t)/(P_0 A/\tau)$.

27

and

$$E_L(t) = \begin{cases} \dfrac{(P_0 A)^2}{2C} \ \dfrac{CC_L}{(C + C_L)^2} \ \dfrac{\left(\dfrac{2r_0}{\ell} + \dfrac{t}{\tau}\right)^2}{\left(\dfrac{2r_0}{\ell} + 1\right)^2} \ \left(\dfrac{t}{\tau}\right)^2 & , \quad 0 \leqslant t \leqslant \tau, \\[20pt] \dfrac{(P_0 A)^2}{2C} \ \dfrac{CC_L}{(C + C_L)^2} \ \left(\dfrac{t}{\tau}\right)^2 & , \qquad t > \tau. \end{cases} \tag{51}$$

The total circuit energy is

$$E_T(t) = \begin{cases} \dfrac{(P_0 A)^2}{2C} \left(\dfrac{C}{C + C_L}\right) \ \dfrac{\left(\dfrac{2r_0}{\ell} + \dfrac{t}{\tau}\right)^2}{\left(\dfrac{2r_0}{\ell} + 1\right)^2} \ \left(\dfrac{t}{\tau}\right)^2 & , \quad 0 \leqslant t \leqslant \tau, \\[20pt] \dfrac{(P_0 A)^2}{2C} \left(\dfrac{C}{C + C_L}\right) & , \qquad t > \tau. \end{cases} \tag{52}$$

Figure 11 contains the normalized energy equations for the hollow-cylinder unit for $r_0/\ell = 1$. The only difference between the energy equations for the hollow-cylinder unit (Equations (50) through (52)) and those for the rectangular unit (Equations (43) through (45)) is the square of the geometrical factor.

V. INDUCTIVE LOAD

A. GENERAL CIRCUIT EQUATIONS

In this section, the load in Figures 1(a) and 1(b) is an inductance L. In this case, the charge will oscillate between the source capacitance and load inductance for all time t. Experiments with inductive loads have shown that dielectric relaxation
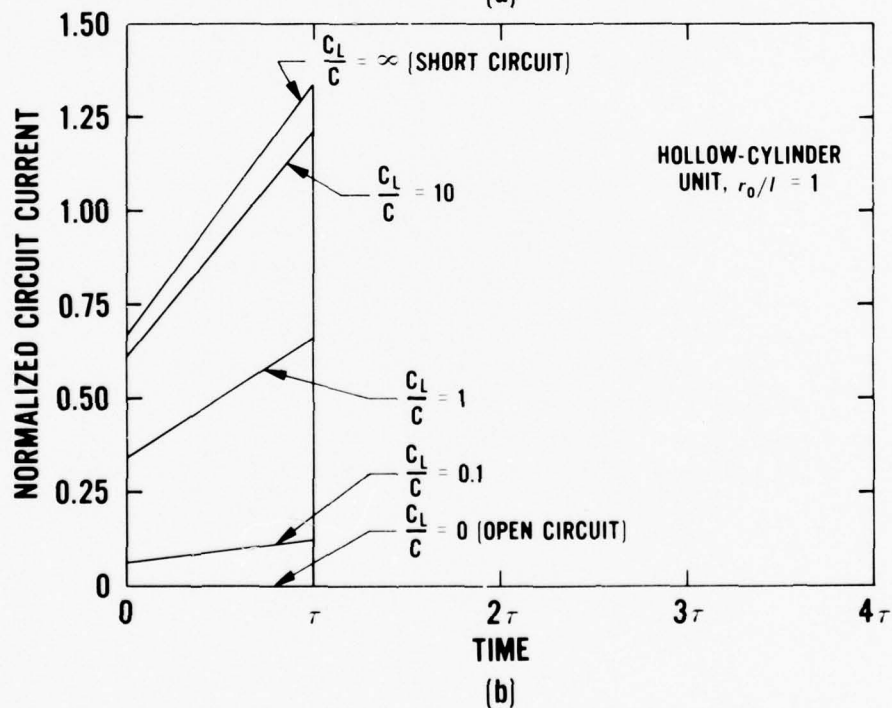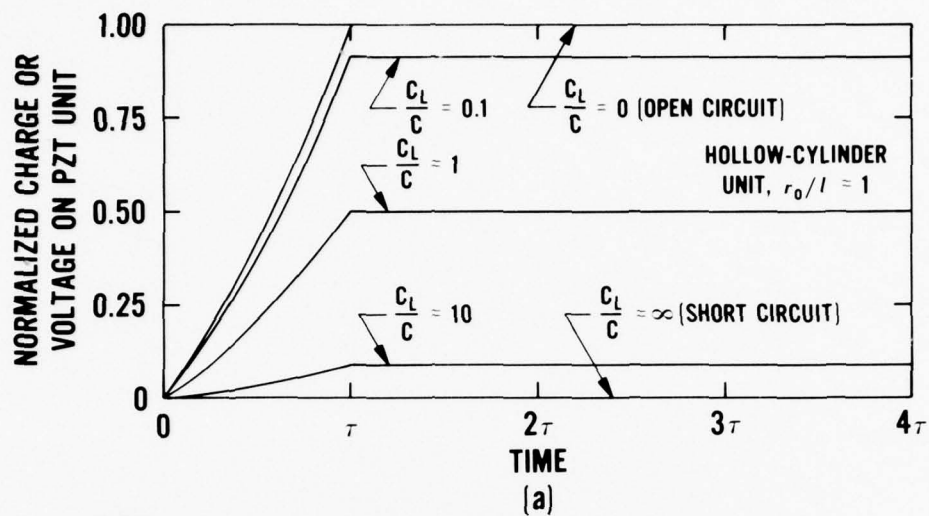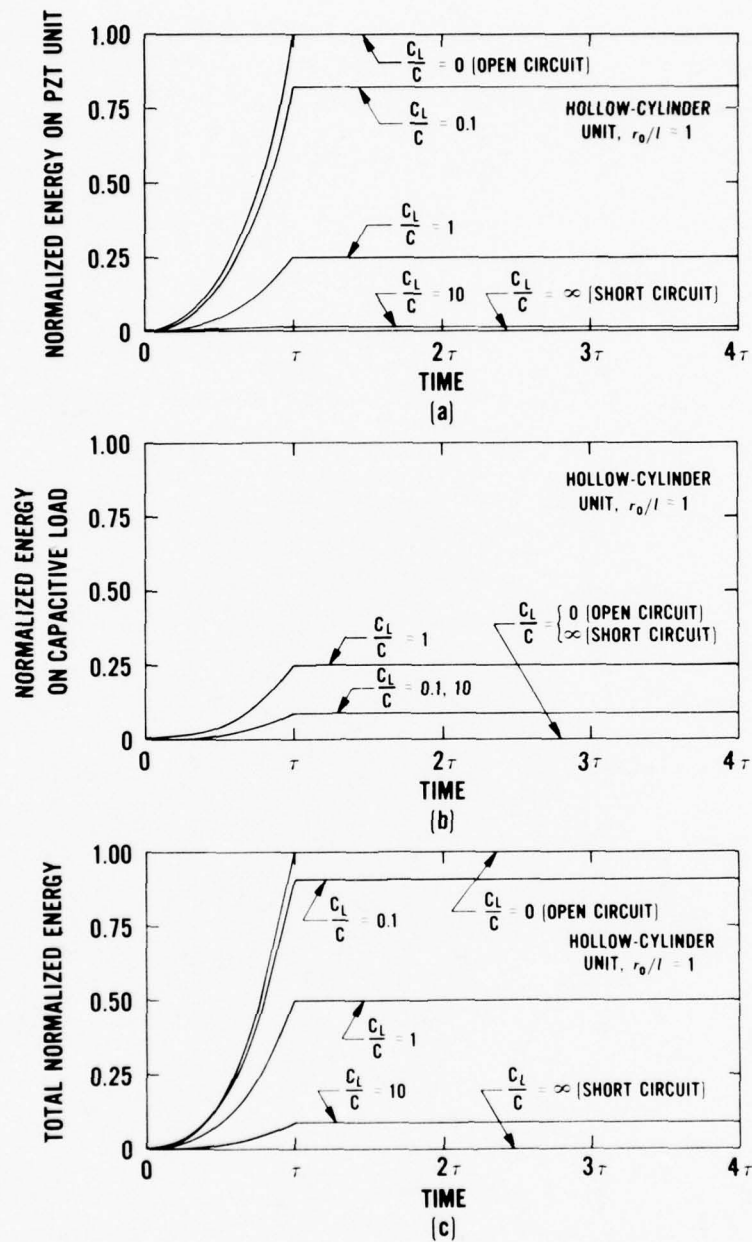
Figure 11. Energy relations for a hollow-cylinder PZT unit with a capacitive load for various values of C_L/C. Curves are given for $r_0/\ell = 1$. (a) Normalized energy $E_C(t)/((P_0A)^2/2C)$ on the PZT unit. (b) Normalized energy $E_L(t)/((P_0A)^2/2C)$ on the capacitive load. (c) Total normalized energy $E_T(t)/((P_0A)^2/2C)$.

29

in PZT 95/5 causes severe damping of the circuit current.[5] Nevertheless an analysis is presented for the idealized case for completeness. Experiments with other PZT materials may be in closer agreement with the simple theory.

The voltage balance equation is

$$\frac{q_c(t)}{C} = L\frac{di(t)}{dt} \quad , \quad t \geqslant 0 . \tag{53}$$

Substituting $di(t)/dt$ from equation (10) gives the differential equation

$$\frac{d^2 q_c(t)}{dt^2} + \frac{q_c(t)}{LC} = \frac{d^2 q(t)}{dt^2} \quad , \quad t \geqslant 0 . \tag{54}$$

This equation is solved for $q_c(t)$ by substituting $q(t)$ from Equation (1) or (5). Also from Equation (10), the current is

$$i(t) = \frac{dq(t)}{dt} - \frac{dq_c(t)}{dt} \quad , \quad t \geqslant 0 . \tag{55}$$

B. RECTANGULAR PZT UNIT

Using Equation (1) for $q(t)$ gives $d^2 q(t)/dt^2 = 0$ for all t. Equation (54) then becomes

$$\frac{d^2 q_c(t)}{dt^2} + \frac{q_c(t)}{LC} = 0 \quad , \quad t \geqslant 0 . \tag{56}$$

This equation is first solved for the range $0 \leqslant t \leqslant \tau$ using the initial conditions $q_c(0) = i(0) = 0$. From Equation (55), $i(t)$ is then obtained. To find $q_c(t)$ and $i(t)$ for $t > \tau$, a general solution is obtained for $q_c(t)$ from Equation (56), then the current is obtained from the equation $i(t) = -dq_c(t)/dt$ (Since $dq(t)/dt = 0$ for $t > \tau$). The continuity of charge and current at $t = \tau$ is used to obtain the two constants in the general solution. This procedure gives

30

$$q_c(t) = \begin{cases} \dfrac{P_0 A}{\omega \tau} \sin \omega t \ , & 0 \leqslant t \leqslant \tau \ , \\[3mm] \dfrac{P_0 A}{\omega \tau} [\sin \omega t - \sin(\omega t - \omega \tau)] \ , & t > \tau \ , \end{cases} \tag{57}$$

and

$$i(t) = \begin{cases} \dfrac{P_0 A}{\tau} (1 - \cos \omega t) \ , & 0 \leqslant t \leqslant \tau \ , \\[3mm] \dfrac{P_0 A}{\tau} [\cos(\omega t - \omega \tau) - \cos \omega t] \ , & t > \tau \ . \end{cases} \tag{58}$$

In these equations ω is the oscillatory frequency given by $\omega^2 = (LC)^{-1}$. Using trigonometric identities to simplify the $q_c(t)$ and $i(t)$ expressions gives

$$q_c(t) = \begin{cases} \dfrac{P_0 A}{\left(\dfrac{\omega \tau}{2}\right)} \sin\left(\dfrac{\omega t}{2}\right) \cos\left(\dfrac{\omega t}{2}\right) \ , & 0 \leqslant t \leqslant \tau \ , \\[5mm] \dfrac{P_0 A}{\left(\dfrac{\omega \tau}{2}\right)} \sin\left(\dfrac{\omega \tau}{2}\right) \cos\left(\omega t - \dfrac{\omega \tau}{2}\right) \ , & t > \tau \ , \end{cases} \tag{59}$$

and

$$i(t) = \begin{cases} \dfrac{2 P_0 A}{\tau} \sin^2\left(\dfrac{\omega t}{2}\right) \ , & 0 \leqslant t \leqslant \tau \ , \\[4mm] \dfrac{2 P_0 A}{\tau} \sin\left(\dfrac{\omega \tau}{2}\right) \sin\left(\omega t - \dfrac{\omega \tau}{2}\right) \ , & t > \tau \ . \end{cases} \tag{60}$$

The voltage on the PZT unit is obtained from the equation $V(t) = q_c(t)/C$. Plots of the normalized charge and voltage are given in Figure 12(a); the normalized current is given in Figure 12(b). $T = 2\pi/\omega$ is the period of oscillation. For the open-circuit case, the oscillatory frequency is zero ($\omega \tau = 0$) and the period of oscillation is infinite ($T/\tau = \infty$). For this case $q_c(t) = q(t)$ and $i(t) = 0$ for all t. This can be shown for $\omega \tau \to 0$ by using the relationships $\sin(\omega t/2)/\omega \tau \to t/2\tau$, $\cos(\omega t/2) \to 1$, and $\cos(\omega t - \omega \tau/2) \to 1$ in Equation (59) for $q_c(t)$, and $\sin(\omega t/2)/\tau \to 0$ in Equation (60) for $i(t)$. As the oscillatory frequency increases, the vibrational amplitude for the normalized charge and voltage decreases. For the short-circuit condition ($\omega \tau = \infty$),
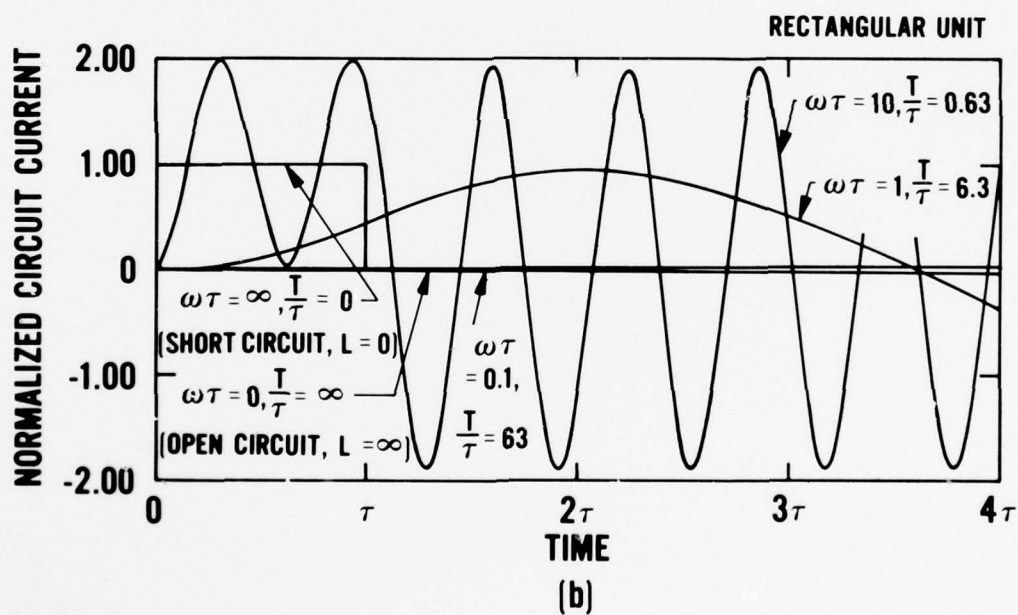
31

Figure 12. Electrical relations for a rectangular PZT unit with an inductive load for various values of $\omega\tau$ or T/τ. (a) Normalized charge $q_c(t)/P_0 A$ or voltage $V(t)/(P_0 A/C)$ on the PZT unit. (b) Normalized circuit current $i(t)/(P_0 A/\tau)$.

32

the frequency of oscillation approaches infinity, but the amplitude of oscillation approaches zero. For this case, it can be shown that $q_c(t) = 0$ for all t by using the relationships $\sin(\omega t/2)/\omega\tau \to 0$ and $\sin(\omega\tau/2)/\omega\tau \to 0$ for $\omega\tau \to \infty$ in Equation (59). For $0 \leqslant t \leqslant \tau$ the current oscillates about $P_0 A/\tau$ with amplitude $P_0 A/\tau$; for $t > \tau$ the current oscillates about a zero value with a variable amplitude $(2P_0 A/\tau)\sin(\omega\tau/2)$. When $\omega\tau$ is an odd multiple of π, the amplitude is $2P_0 A/\tau$. When $\omega\tau$ is an even multiple of π, the amplitude is zero. The short-circuit current ($\omega\tau = \infty$) can be obtained from Equation (55) using $q_c(t) = 0$ for all t, or from Equation (60) using $\sin^2(\omega t/2) \to 1/2$ and $\sin(\omega\tau/2) \to 0$ as $\omega\tau \to \infty$. As expected the result is

$$
i(t,\omega\tau = \infty) = \begin{cases} \dfrac{P_0 A}{\tau} & , \quad 0 \leqslant t. \leqslant \tau , \\[2em] 0 & , \quad\quad t > \tau . \end{cases} \tag{61}
$$

Expressions for the energy on the PZT unit and load inductance can be obtained, respectively, from the equations $E_c(t) = q_c^2(t)/2C$ and $E_L(t) = L\,i^2(t)/2$.

The results are

$$
E_C(t) = \begin{cases} \dfrac{(P_0 A)^2}{2C} \left[\dfrac{\sin\left(\dfrac{\omega t}{2}\right)\cos\left(\dfrac{\omega t}{2}\right)}{\dfrac{\omega\tau}{2}} \right]^2 & , \quad 0 \leqslant t \leqslant \tau , \\[3em] \dfrac{(P_0 A)^2}{2C} \left[\dfrac{\sin\left(\dfrac{\omega\tau}{2}\right)\cos\left(\omega t - \dfrac{\omega\tau}{2}\right)}{\dfrac{\omega\tau}{2}} \right]^2 & , \quad\quad t > \tau , \end{cases} \tag{62}
$$

and

$$
E_L(t) = \begin{cases} \dfrac{(P_0 A)^2}{2C} \left[\dfrac{\sin\left(\dfrac{\omega\tau}{2}\right)}{\dfrac{\omega\tau}{2}} \right]^2 & , \quad 0 \leqslant t \leqslant \tau , \\[3em] \dfrac{(P_0 A)^2}{2C} \left[\dfrac{\sin\left(\dfrac{\omega\tau}{2}\right)\sin\left(\omega t - \dfrac{\omega\tau}{2}\right)}{\dfrac{\omega\tau}{2}} \right]^2 & , \quad t > \tau . \end{cases} \tag{63}
$$

The expression for the total circuit energy $E_T(t) = E_C(t) + E_L(t)$ is

$$E_T(t) = \begin{cases} \dfrac{(P_0 A)^2}{2C}\left[\dfrac{\sin\left(\dfrac{\omega t}{2}\right)}{\dfrac{\omega\tau}{2}}\right]^2 , & 0 \leqslant t \leqslant \tau, \\[3em] \dfrac{(P_0 A)^2}{2C}\left[\dfrac{\sin\left(\dfrac{\omega\tau}{2}\right)}{\dfrac{\omega\tau}{2}}\right]^2 , & t > \tau. \end{cases} \tag{64}$$

Figures 13(a), 13(b), and 13(c) are plots of the normalized energy expressions for various values of the parameter $\omega\tau$. For the open-circuit condition ($\omega\tau = 0$), it can be shown that $E_T(t) = [(P_0 A)^2/2C](t/\tau)^2$ for $0 \leqslant t \leqslant \tau$ and $E_T(t) = (P_0 A)^2/2C$ for $t > \tau$, and that $E_L(t) = 0$ for all t. Also, for the short-circuit condition ($\omega\tau = \infty$), $E_C(t) = E_L(t) = E_T(t)$ for all t. Figures 13(a), 13(b), and 13(c) indicate that for $0 \leqslant t \leqslant \tau$ the PZT, inductive, and total energies are oscillatory in nature. For $t > \tau$, the total circuit energy is constant, but it oscillates between the PZT unit and inductance with frequency ω. This situation can be compared with the capacitive load in which the energies on the PZT unit and load capacitance remained fixed for $t > \tau$. The total energy curves for $\omega\tau = 0$ and $\omega\tau = 0.1$ are within about 0.1% of each other and, therefore, could not be shown as separated on the plot.

For $t = \tau$ and $\omega\tau = 1$ (Figure 13(a)), the normalized PZT energy is about 70% of the maximum theoretical value. At $t = 2.1\tau$, the PZT energy is zero (corresponding to the case of zero charge and voltage on the PZT unit and maximum circuit current (see Figures 12(a) and 12(b)), but at about $t = 2.65\tau$ the PZT energy has increased to about 90%, since, at this time the energy that was on the inductor at $t = \tau$ (about 20%) has been transferred back to the PZT unit. For this case, considerable charge (about $0.95\,P_0 A$) is being transferred back and forth between the PZT unit and inductance (Figure 12(a)). The inductive energy is about 90% of the theoretical maximum value at $t = 2.1\tau$. (This corresponds to the case of zero capacitive energy.) This inductive energy transfer is greater than the 25% maximum energy transfer for the capacitive load (Figure 9(b)).

Note that in Figure 13(b) the $\omega\tau = 1$ curve peaked at $t = 2.1\tau$. As $\omega\tau$ decreases from this value, the amplitude of the curve increases, and the peak occurs for larger times. For $\omega\tau = 0.1$, the amplitude of the peak is 99% of the theoretical maximum value and occurs at $t = 164\tau$. As $\omega\tau$ increases from $\omega\tau = 1$, the amplitude of the peak decreases and occurs for smaller times. The result for $\omega\tau = 10$ is shown in the figure.
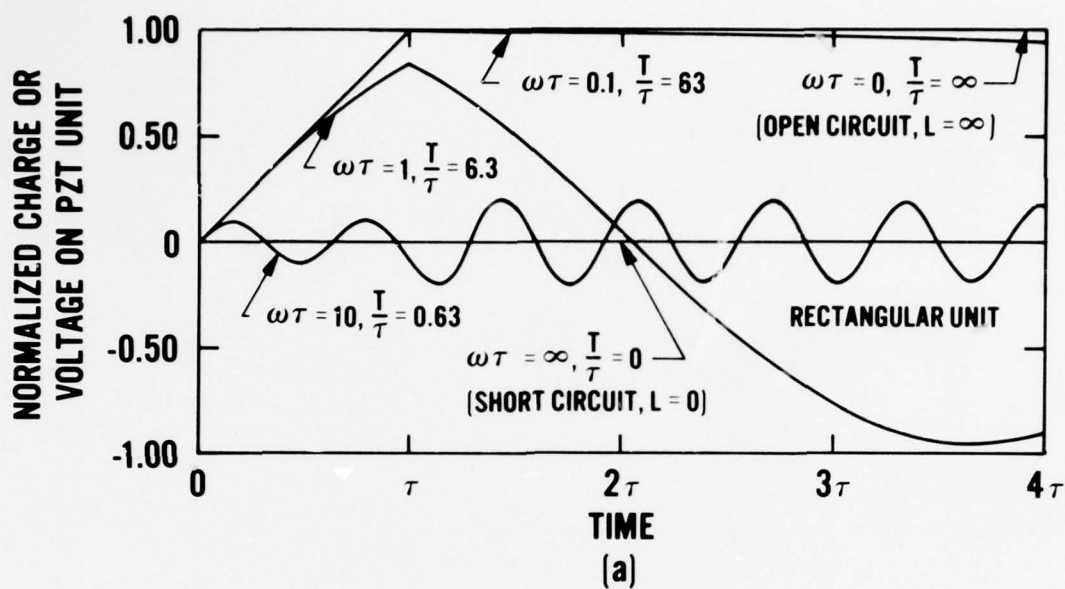
34
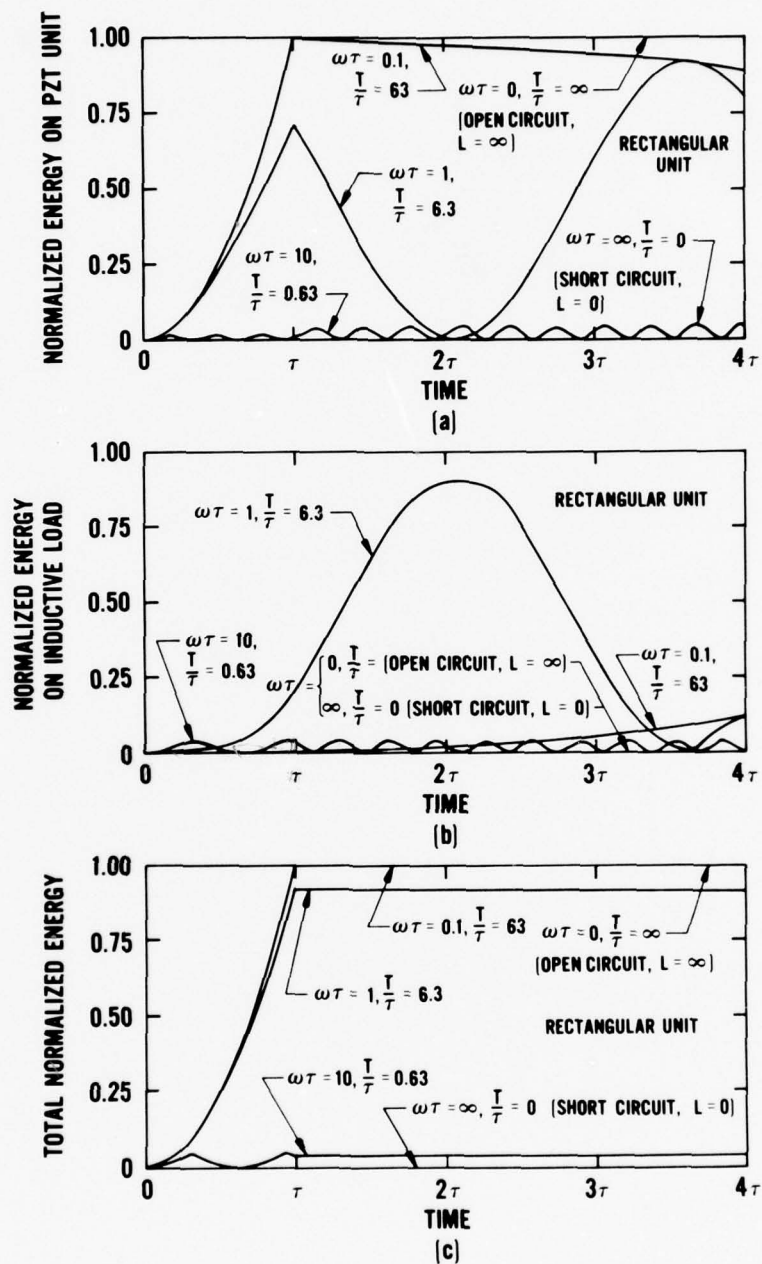
Figure 13. Energy relations for a rectangular PZT unit with an inductive load for various values of $\omega\tau$ or T/τ. (a) Normalized energy $E_C(t)/((P_0A)^2/2C)$ on the PZT unit. (b) Normalized energy $E_L(t)/((P_0A)^2/2C)$ on the inductive load. (c) Total normalized energy $E_T(t)/((P_0A)^2/2C)$.

35

C. HOLLOW-CYLINDER PZT UNIT

Substituting $d^2 q(t)/dt^2$ from Equation (5) into Equation (54) gives the differential equations for $q_c(t)$,

$$\frac{d^2 q_c(t)}{dt^2} + \frac{q_c(t)}{LC} = \frac{2P_0 A}{\tau^2 \left(\frac{2r_0}{\ell} + 1 \right)} , \quad 0 \le t \le \tau , \tag{65}$$

and

$$\frac{d^2 q_c(t)}{dt} + \frac{q_c(t)}{LC} = 0 \quad , \quad t > \tau . \tag{66}$$

The same procedure is used for solving these equations and Equation (55) for $q_c(t)$ and $i(t)$ that was used for solving the equations for the rectangular PZT unit. This procedure gives

$$q_c(t) = \begin{cases} \dfrac{P_0 A}{\omega \tau} \dfrac{\left(\frac{2r_0}{\ell} \right)}{\left(\frac{2r_0}{\ell} + 1 \right)} \left[\sin \omega t + \dfrac{1}{\omega \tau \left(\frac{r_0}{\ell} \right)} (1 - \cos \omega t) \right] , \quad 0 \le t \le \tau , \\[4mm] \dfrac{P_0 A}{\omega \tau} \dfrac{\left(\frac{2r_0}{\ell} \right)}{\left(\frac{2r_0}{\ell} + 1 \right)} \left[\sin \omega t - \sin(\omega t - \omega \tau) + \dfrac{1}{\omega \tau \left(\frac{r_0}{\ell} \right)} [\cos(\omega t - \omega \tau) - \cos \omega t] - \dfrac{1}{\left(\frac{r_0}{\ell} \right)} \sin(\omega t - \omega \tau) \right] , \ t > \tau , \end{cases} \tag{67}$$

36

and

$$i(t) = \begin{cases} \dfrac{P_0 A}{\tau} \dfrac{\left(\dfrac{2r_0}{\varrho}\right)}{\left(\dfrac{2r_0}{\varrho}+1\right)} \left[(1-\cos\omega t) - \dfrac{1}{\omega t \left(\dfrac{r_0}{\varrho}\right)}\sin\omega t + \dfrac{1}{\left(\dfrac{r_0}{\varrho}\right)}\left(\dfrac{t}{\tau}\right)\right], & 0 \le t \le \tau, \\[20pt] \dfrac{P_0 A}{\tau} \dfrac{\left(\dfrac{2r_0}{\varrho}\right)}{\left(\dfrac{2r_0}{\varrho}+1\right)} \left[\cos(\omega t - \omega\tau) - \cos\omega t + \dfrac{1}{\omega t \left(\dfrac{r_0}{\varrho}\right)}[\sin(\omega t - \omega\tau) - \sin\omega t] + \dfrac{1}{\left(\dfrac{r_0}{\varrho}\right)}\cos(\omega t - \omega\tau)\right], & t > \tau. \end{cases}$$ (68)

Using trigonometric identities gives

$$q_c(t) = \begin{cases} \dfrac{P_0 A}{\left(\dfrac{\omega\tau}{2}\right)} \dfrac{\left(\dfrac{2r_0}{\varrho}\right)}{\left(\dfrac{2r_0}{\varrho}+1\right)} \left[\sin\!\left(\dfrac{\omega t}{2}\right)\cos\!\left(\dfrac{\omega t}{2}\right) + \dfrac{1}{\omega\tau\left(\dfrac{r_0}{\varrho}\right)}\sin^2\!\left(\dfrac{\omega t}{2}\right)\right], & 0 \le t \le \tau, \\[20pt] \dfrac{P_0 A}{\left(\dfrac{\omega\tau}{2}\right)} \dfrac{\left(\dfrac{2r_0}{\varrho}\right)}{\left(\dfrac{2r_0}{\varrho}+1\right)} \left[\sin\!\left(\dfrac{\omega\tau}{2}\right)\cos\!\left(\omega t - \dfrac{\omega\tau}{2}\right) + \dfrac{1}{\omega t\left(\dfrac{r_0}{\varrho}\right)}\sin\!\left(\dfrac{\omega\tau}{2}\right)\sin\!\left(\omega t - \dfrac{\omega\tau}{2}\right) - \dfrac{1}{\left(\dfrac{2r_0}{\varrho}\right)}\sin(\omega t - \omega\tau)\right], & t > \tau, \end{cases}$$ (69)

and

$$i(t) = \begin{cases} \dfrac{2P_0 A}{\tau} \dfrac{\left(\dfrac{2r_0}{\varrho}\right)}{\left(\dfrac{2r_0}{\varrho}+1\right)} \left[\sin^2\!\left(\dfrac{\omega t}{2}\right) - \dfrac{1}{\omega t \left(\dfrac{r_0}{\varrho}\right)}\sin\!\left(\dfrac{\omega t}{2}\right)\cos\!\left(\dfrac{\omega t}{2}\right) + \dfrac{1}{\left(\dfrac{2r_0}{\varrho}\right)}\left(\dfrac{t}{\tau}\right)\right], & 0 \le t \le \tau, \\[20pt] \dfrac{2P_0 A}{\tau} \dfrac{\left(\dfrac{2r_0}{\varrho}\right)}{\left(\dfrac{2r_0}{\varrho}+1\right)} \left[\sin\!\left(\dfrac{\omega\tau}{2}\right)\sin\!\left(\omega t - \dfrac{\omega\tau}{2}\right) - \dfrac{1}{\omega t \left(\dfrac{r_0}{\varrho}\right)}\sin\!\left(\dfrac{\omega\tau}{2}\right)\cos\!\left(\omega t - \dfrac{\omega\tau}{2}\right) + \dfrac{1}{\left(\dfrac{2r_0}{\varrho}\right)}\cos(\omega t - \omega\tau)\right], & t > \tau. \end{cases}$$ (70)

Plots of the normalized charge and voltage are given in Figure 14(a) for $r_0/\varrho = 1$; the normalized charge is given in Figure 14(b).

37

NORMALIZED CHARGE OR VOLTAGE ON PZT UNIT

1.00

0.50

0

-0.50

-1.00

$\omega\tau = 0.1, \frac{T}{\tau} = 63$

$\omega\tau = 1, \frac{T}{\tau} = 6.3$

$\omega\tau = 0, \frac{T}{\tau} = \infty$

(OPEN CIRCUIT, L = ∞)

$\omega\tau = 10, \frac{T}{\tau} = 0.63$

$\omega\tau = \infty, \frac{T}{\tau} = 0$

(SHORT CIRCUIT, L = 0)

HOLLOW-CYLINDER
UNIT, $r_0/l = 1$

0   τ 2τ 3τ 4τ

TIME

(a)

HOLLOW-CYLINDER
UNIT, $r_0/l = 1$

NORMALIZED CIRCUIT CURRENT

2.00

1.00

0

-1.00

-2.00

$\omega\tau = 10, \frac{T}{\tau} = 0.63$

$\omega\tau = 1, \frac{T}{\tau} = 6.3$

$\omega\tau = \infty, \frac{T}{\tau} = 0$

(SHORT CIRCUIT,
L = 0)

$\omega\tau = 0, \frac{T}{\tau} = \infty$

(OPEN CIRCUIT, L = ∞)

$\omega\tau = 0.1, \frac{T}{\tau} = 63$

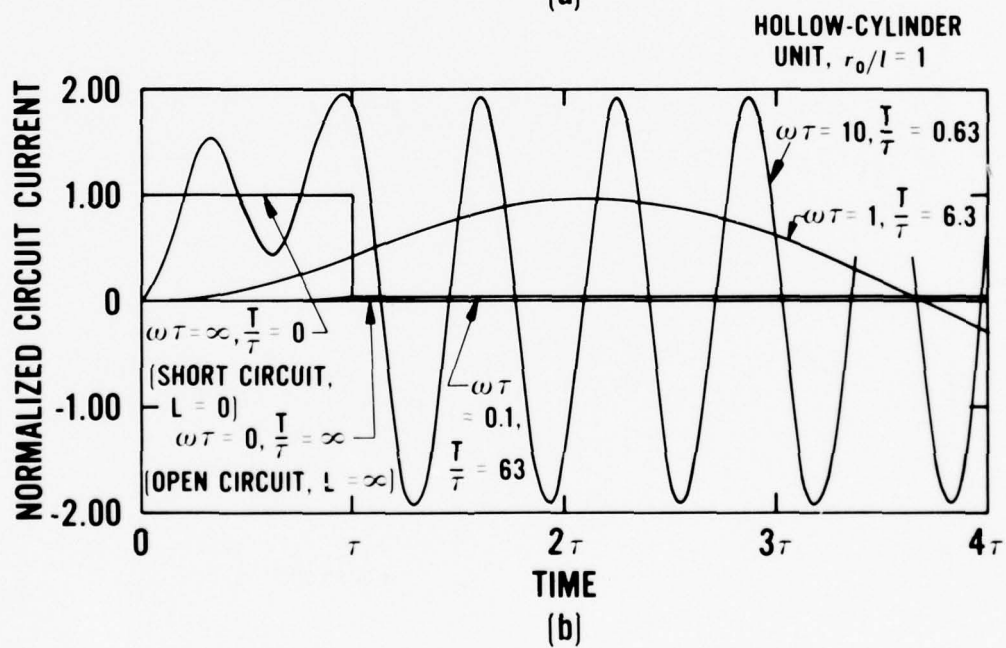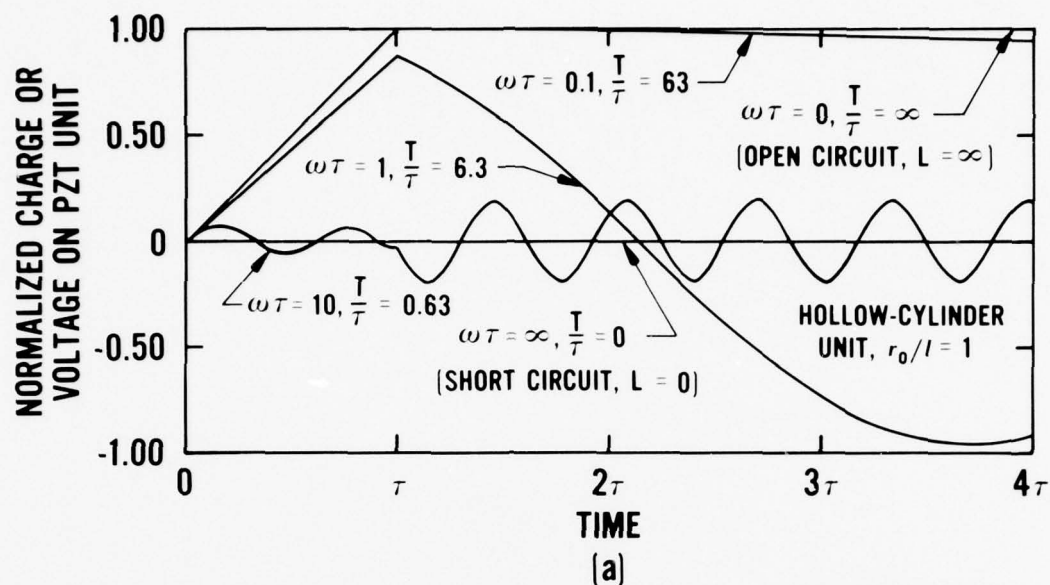0 τ 2τ 3τ 4τ

TIME

(b)

Figure 14. Electrical expressions for a hollow-cylinder PZT unit with an inductive load for various values of $\omega\tau$ or T/τ. Curves are given for $r_0/\ell = 1$. (a) Normalized charge $q_c(t)/P_0 A$ or voltage $V(t)/(P_0 A/C)$ on the PZT unit. (b) Normalized circuit current $i(t)/(P_0 A/\tau)$.

38

Equations (69) and (70) are both continuous at $t = \tau$. Also, these equations reduce to Equations (59) and (60), respectively, for the rectangular PZT unit as $r_0/\ell \to \infty$. Since $(2r_0/\ell)/[(2r_0/\ell) + 1] \to 1$, and $1/(r_0/\ell) \to 0$, as $r_0/\ell \to \infty$, only the first terms in Equations (69) and (70) are nonzero, and these are just the terms in Equations (59) and (60) for the rectangular PZT unit.

For the open-circuit case ($\omega\tau = 0$), the limiting values as $\omega\tau \to 0$ for the trigonometric relationships given in the previous section for the rectangular unit can be used to show that Equations (69) and (70) become, respectively,

$$q_c(t,\omega\tau = 0) = \begin{cases} P_0 A \dfrac{\left(\dfrac{2r_0}{\ell} + \dfrac{t}{\tau}\right)}{\left(\dfrac{2r_0}{\ell} + 1\right)} \left(\dfrac{t}{\tau}\right), & 0 \leqslant t \leqslant \tau, \\[20pt] P_0 A & t > \tau, \end{cases} \tag{71}$$

and

$$i(t,\omega\tau = 0) = 0 \quad , \quad t \geqslant 0. \tag{72}$$

Equation (71) is just the charge release $q(t)$ from a hollow-cylinder PZT unit (Equation (5)).

For the short-circuit case ($\omega\tau = \infty$), the relationships $\sin(\omega t/2) \to 0$, $\sin^2(\omega t/2) \to 1/2$ as $\omega\tau \to \infty$ can be used to show that Equations (69) and (70) reduce to

$$q_c(t,\omega\tau = \infty) = 0 \quad , \quad t \geqslant 0, \tag{73}$$

and

$$i(t,\omega\tau = \infty) = \begin{cases} \dfrac{P_0 A}{\tau} \dfrac{\left(\dfrac{2r_0}{\ell} + \dfrac{2t}{\tau}\right)}{\left(\dfrac{2r_0}{\ell} + 1\right)}, & 0 \leqslant t \leqslant \tau, \\[20pt] 0 & t > \tau. \end{cases} \tag{74}$$

As expected, the short-circuit current in Equation (74) agrees with the short-circuit current for the resistive load (Equation (27)) and capacitive load (Equation (49)) with $C_L/C = \infty$). The voltage on the hollow-cylinder unit can be obtained by substituting $q_c(t)$ from Equation (69) into the equation $V(t) = q_c(t)/C$.

Expressions for the energy on the PZT unit and inductance are obtained, respectively, from $E_C(t) = q_c^2(t)/2C$ and $E_L(t) = L\,i^2(t)/2$. Making substitutions for $q_c(t)$ from Equation (69) and $i(t)$ from Equation (70) gives

$$
E_C(t) = \begin{cases}
\dfrac{(P_0 A)^2}{2C} \dfrac{\left(\frac{2r_0}{\ell}\right)^2}{\left(\frac{2r_0}{\ell}+1\right)^2} \left[\dfrac{\sin\left(\frac{\omega t}{2}\right)\cos\left(\frac{\omega t}{2}\right) + (\omega\tau)^{-1}\left(\frac{r_0}{\ell}\right)^{-1}\sin^2\left(\frac{\omega t}{2}\right)}{\frac{\omega\tau}{2}}\right]^2 , & 0 \le t \le \tau, \\[4ex]
\dfrac{(P_0 A)^2}{2C} \dfrac{\left(\frac{2r_0}{\ell}\right)^2}{\left(\frac{2r_0}{\ell}+1\right)^2} \left[\dfrac{\sin\left(\frac{\omega\tau}{2}\right)\cos\left(\omega t - \frac{\omega\tau}{2}\right) + (\omega\tau)^{-1}\left(\frac{r_0}{\ell}\right)^{-1}\sin\left(\frac{\omega\tau}{2}\right)\sin\left(\omega t - \frac{\omega\tau}{2}\right) - 1/2\left(\frac{r_0}{\ell}\right)^{-1}\sin(\omega t - \omega\tau)}{\frac{\omega\tau}{2}}\right]^2 , & t > \tau,
\end{cases}
\tag{75}
$$

and

$$
E_L(t) = \begin{cases}
\dfrac{(P_0 A)^2}{2C} \dfrac{\left(\frac{2r_0}{\ell}\right)^2}{\left(\frac{2r_0}{\ell}+1\right)^2} \left[\dfrac{\sin^2\left(\frac{\omega t}{2}\right) - (\omega\tau)^{-1}\left(\frac{r_0}{\ell}\right)^{-1}\sin\left(\frac{\omega t}{2}\right)\cos\left(\frac{\omega t}{2}\right) + 1/2\left(\frac{r_0}{\ell}\right)^{-1}\left(\frac{t}{\tau}\right)}{\frac{\omega\tau}{2}}\right]^2 , & 0 \le t \le \tau, \\[4ex]
\dfrac{(P_0 A)^2}{2C} \dfrac{\left(\frac{2r_0}{\ell}\right)^2}{\left(\frac{2r_0}{\ell}+1\right)^2} \left[\dfrac{\sin\left(\frac{\omega\tau}{2}\right)\sin\left(\omega t - \frac{\omega\tau}{2}\right) - (\omega\tau)^{-1}\left(\frac{r_0}{\ell}\right)^{-1}\sin\left(\frac{\omega\tau}{2}\right)\cos\left(\omega t - \frac{\omega\tau}{2}\right) + 1/2\left(\frac{r_0}{\ell}\right)^{-1}\cos(\omega t - \omega\tau)}{\frac{\omega\tau}{2}}\right]^2 , & t > \tau.
\end{cases}
\tag{76}
$$

The total circuit energy is obtained by adding Equations (75) and (76), to give

$$
E_T(t) = \begin{cases}
\dfrac{(P_0 A)^2}{2C} \dfrac{\left(\frac{2r_0}{\ell}\right)^2}{\left(\frac{2r_0}{\ell}+1\right)^2} \dfrac{\left[\sin^2\left(\frac{\omega t}{2}\right)\left[1 + \left(\frac{r_0}{\ell}\right)^{-1}\left(\frac{t}{\tau}\right) + (\omega\tau)^{-2}\left(\frac{r_0}{\ell}\right)^{-2}\right] + 1/4\left(\frac{r_0}{\ell}\right)^{-2}\left(\frac{t}{\tau}\right)^2 - (\omega\tau)^{-1}\left(\frac{r_0}{\ell}\right)^{-2}\left(\frac{t}{\tau}\right)\sin\left(\frac{\omega t}{2}\right)\cos\left(\frac{\omega t}{2}\right)\right]}{\left(\frac{\omega\tau}{2}\right)^2} , & 0 \le t \le \tau, \\[4ex]
\dfrac{(P_0 A)^2}{2C} \dfrac{\left(\frac{2r_0}{\ell}\right)^2}{\left(\frac{2r_0}{\ell}+1\right)^2} \dfrac{\left[\sin^2\left(\frac{\omega\tau}{2}\right)\left[1 + (\omega\tau)^{-2}\left(\frac{r_0}{\ell}\right)^{-2} + \left(\frac{r_0}{\ell}\right)^{-1}\right] + 1/4\left(\frac{r_0}{\ell}\right)^{-2} - (\omega\tau)^{-1}\left(\frac{r_0}{\ell}\right)^{-2}\sin\left(\frac{\omega\tau}{2}\right)\cos\left(\frac{\omega\tau}{2}\right)\right]}{\left(\frac{\omega\tau}{2}\right)^2} , & t > \tau.
\end{cases}
\tag{77}
$$

40

These energy expressions are continuous at $t = \tau$. Also, as $r_0/\ell \to \infty$ Equations (75), (76), and (77) reduce to Equations (62), (63), and (64) for the rectangular PZT unit, respectively. Figures 15(a), 15(b), and 15(c) are plots of the normalized energy expressions for $r_0/\ell = 1$.

VI. GEOMETRICAL SIZE ESTIMATES OF PZT UNITS IN FERROELECTRIC POWER SUPPLIES FOR SOME EXAMPLE HIGH-VOLTAGE ENERGY CONVERTERS

In this section, the geometrical size of PZT units for use in pulsed power supplies will be estimated for some example energy converters. Energy converters with resistive and capacitive input impedances were chosen. The electrical equations that were derived in Sections III and IV will be used in the analysis. Expressions for the area A and height h of the PZT unit will be obtained in terms of the converter input resistance R or capacitance C_L and the input voltage V. The shock and electrical parameters for the PZT unit will be taken as those for PZT 56/44 material. A 12.6-mm cube of PZT 56/44 had a capacitance C of 240 pF.[1] For this cube, it was shown experimentally that about 40 μC of the 51 μC of available charge was released at a maximum electric field F_0 of about 2 kV/mm in the 7 to 8 GPa stress range.[1] In this analysis, P_0 will therefore be taken as 0.25 μC/mm^2 (40 μC/(12.6 mm)^2). (The PZT 56/44 remanent polarization vector P_0 is 0.33 μC/mm^2.[1] We have simplified the present analysis by taking P_0 as representing the actual charge released.) The average measured shock velocity U was 4.65 km/s.[1] The geometrical shape of the PZT unit will be discussed after the size has been estimated. It should be noted that in most experiments, stresses from relief wave interactions will have destroyed the unit for times significantly greater than the shock transit time τ.

A. CONVERTERS WITH RESISTIVE INPUT IMPEDANCES

Table 1 lists two converters and their characteristics. These converters require approximately flat-topped input voltage pulses. Figures 2(a) and 4(a) for the rectangular and hollow-cylinder units, respectively, indicate that the value of RC/τ must be near that for short-circuit conditions (0.1 or less) for this type of pulse. The load voltage reaches a constant value soon after the shock wave enters the PZT unit and does not begin to decrease until after the shock wave passes out of the unit. Expressions for the voltage near short-circuit conditions (RC/$\tau \to 0$) can be obtained using $q_c(t)$ from Equation (12) for the rectangular unit and using $q_c(t)$ from Equation (23) for the hollow-cylinder unit in the equation $V(t) = q_c(t)/C$. The results are
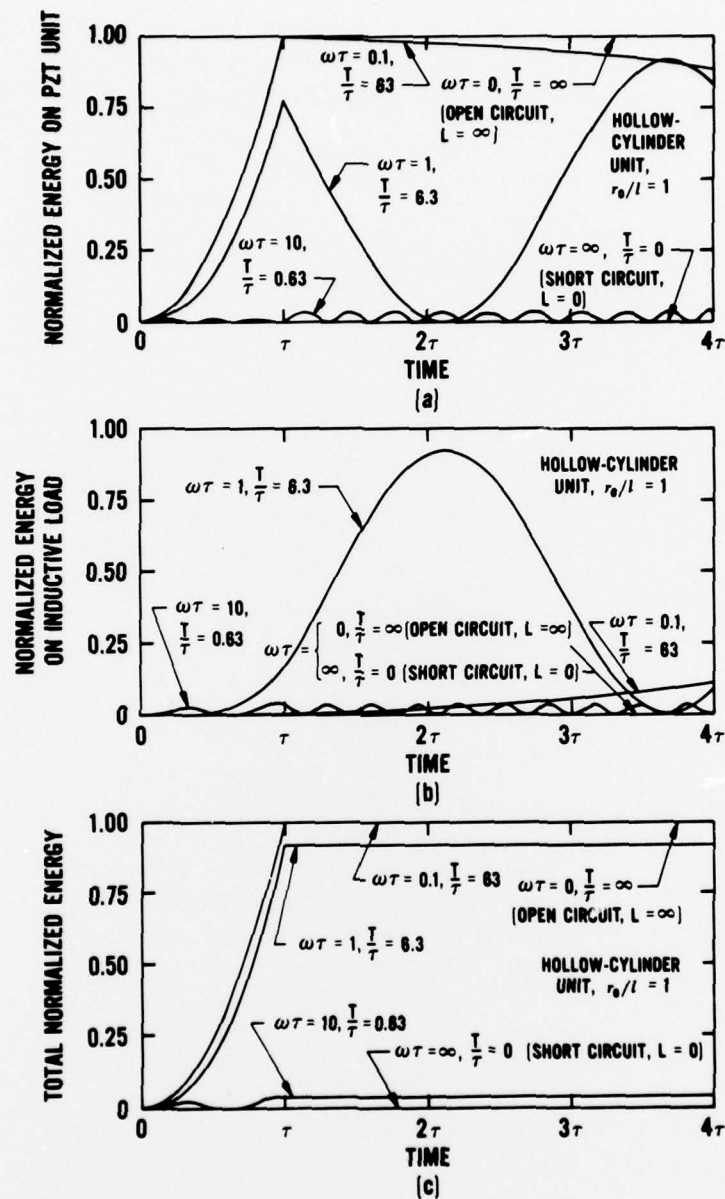
Figure 15. Energy expressions for a hollow-cylinder PZT unit with an inductive load for various values of $\omega\tau$ or T/τ. Curves are given for $r_0/\ell = 1$. (a) Normalized energy $E_C(t)/((P_0A)^2/2C)$ on the PZT unit. (b) Normalized energy $E_L(t)/((P_0A)^2/2C)$ on the inductive load. (c) Total normalized energy $E_T(t)/((P_0A)^2/2C)$.

42

$$V(t,RC/\tau \to 0) = \begin{cases} \dfrac{P_0 A}{C}\left(\dfrac{RC}{\tau}\right), & 0 \leqslant t \leqslant \tau, \\[12pt] 0 & , \quad t > \tau, \end{cases} \qquad (78)$$

for the rectangular unit, and

$$V(t,RC/\tau \to 0) = \begin{cases} \dfrac{P_0 A}{C}\dfrac{\left(\dfrac{2r_0}{\ell} + \dfrac{2t}{\tau}\right)}{\left(\dfrac{2r_0}{\ell} + 1\right)}\left(\dfrac{RC}{\tau}\right), & 0 \leqslant t \leqslant \tau \\[12pt] 0 & , \quad t > \tau, \end{cases} \qquad (79)$$

Table 1. Energy converters with resistive input impedances.[13]

Converter	Input Resistance R (kΩ)	Input Voltage V (kV)	Pulse Duration of Flat-Topped Input Pulse τ (μs)
Magnetron	0.4 - 1	50	0.1 - 10 (use 2.7 μs)[a]
Klystron	0.4 - 2	100 - 1000	(use 2.7 μs)[a]

[a]The 2.7-μs value for the pulse duration is the average transit time τ calculated using a 4.65 km/s shock transit time[1] for PZT 56/44 material and a PZT unit thickness ℓ of 12.6 mm.

for the hollow-cylinder unit. For $r_0/\ell \gg 1$, Equation (79) reduces to Equation (78). Equation (78) will be used for estimating the size of the PZT unit. Figure 2(a) for $RC/\tau = 0.1$ indicates that the normalized charge and voltage are about 10% of their maximum values. This is also indicated in Equation (78) by substituting 0.1 for RC/τ.

The height h, thickness ℓ, and width w for the PZT unit can be calculated using Equation (78) for V and the electrical and shock characteristics of the PZT 56/44 material.

The height h is given by

$$h = V/F_0 \tag{80}$$

where $F_0 = 2$ kV/mm and V is the applied voltage. The thickness ℓ is given by

$$\ell = U\tau \tag{81}$$

where $U = 4.65$ km/s and τ is the required input pulse duration. The width w obtained from Equations (78) and (81) is

$$w = \frac{V}{RP_0 U} \tag{82}$$

where R is the converter input impedance and $P_0 = 0.25$ μC/mm^2. If 240 pF is the capacitance of a 12.6-mm PZT 56/44 cube, then

$$C = 0.019 \frac{A}{h} \tag{83}$$

is the capacitance in nF of a PZT 56/44 unit with area A in mm^2 and height h in mm.

The dimensionless parameter RC/τ in Equation (78) can be obtained using V from Equation (80) and C from Equation (83). The result is

$$\frac{RC}{\tau} = 0.019 \frac{F_0}{P_0} = 0.15 \tag{84}$$

where the values for F_0 and P_0 have been used. For this value of RC/τ about 15% of the available charge will remain on the PZT unit and 85% flow through the resistive load (Figure 2(a)). At $t = \tau$, the energy $E_L(\tau)$ dissipated in the load resistance R is given by

44

$$E_L(\tau) = \frac{V^2 \tau}{R} \ . \tag{85}$$

This can be shown using i = V/R in the equation $E_L(t) = \int_0^\tau i^2(t)dt$.

In the analysis to follow, the thickness ℓ of the PZT unit will be taken to be 12.6 mm giving a pulse duration τ of 2.7 μs. This thickness was chosen because it corresponds to a measured charge release of about 77%.[1] If a different thickness were used, then the charge release may be different, requiring a P_0 different from 0.25 μC/mm^2 in the calculations.

Table 2 gives the PZT geometrical size estimates for the energy converters. The input resistances and voltages were chosen to cover the range of input characteristics in Table 1. The size estimates for the magnetron indicate that a single rectangular unit or a series of rectangular units connected electrically in parallel would provide a reasonable power source. In Reference 1, a shock-depoled PZT 56/44 unit 25.9-mm high, 25.6-mm wide, and 12.4-mm long (unit volume 8 cm^3) was used to pulse charge a 1.2 nF load capacitor to 55 kV. About 78% of the available charge was released. This unit is similar in size to the estimated PZT units for the magnetron in Table 2. The size estimates for the klystron indicate that hollow-cylinder units may be more appropriate than rectangular units due to the large amount of PZT material required. Also, the large height of PZT material (500 mm) for the 1000-kV input voltage may be prohibitive due to the extreme care that would be required during fabrication of the unit from the PZT elements.

Note that in the calculations for Table 2 the height h and width w are determined from the input resistance and voltage, but the length ℓ depends only on the pulse duration τ. A change in τ affects the volume of PZT material required to drive the converters, but not the shape of the voltage pulse since RC/τ is constant. Also, as expected, changing τ also changes the energy dissipated in the resistance (Equation (85)).

B. CONVERTERS WITH CAPACITIVE INPUT IMPEDANCES

Table 3 lists five converters and their characteristics. Expressions for the area A and height h of the PZT unit will be calculated in terms of the converter input capacitance C_L and input voltage V. The voltage on the PZT unit and converter for t = τ will be used for estimating the size of the unit. Equations (41) and (48) are

45

Table 2. Estimated geometrical and electrical characteristics of PZT units for energy converters with resistive input impedances.

Energy Converter	Input Resistance R (kΩ)	Input Voltage V (kV)	Pulse Duration τ (μs)	Unit Height h[a] (mm)	Unit Length[b] (mm)	Unit Width w[c] (mm)	Unit Area A (mm²)	Inner Cylinder Diameter d_0[d] (mm)	Geometrical Ratio[e] r_0/ℓ	Unit Volume (cm³)	Unit Mass[f] (kg)	Unit Capacitance C[g] (nF)	Unit Charge P_0A (μC)	RC Time Constant (μs)	Time Parameter RC/τ
Magnetron	0.4	50	2.7	25	12.6	110	1400	22	0.9	34	0.26	1.0	340	0.41	0.15
	1	50	2.7	25	12.6	43	540	1.0[h]	0.04	14	0.10	0.41	140	0.41	0.15
Klystron	0.4	100	2.7	50	12.6	220	2700	56	2.2	140	1.0	1.0	680	0.41	0.15
	2	1000	2.7	500	12.6	430	5400	124	4.9	2700	21	0.21	1400	0.41	0.15

a Calculated using Equation (80).

b Taken as 12.6 mm.

c Calculated using Equation (82).

d Inner diameter of hollow-cylinder unit having a cross-sectional area A, height h, and a wall thickness $\ell = 12.6$ mm $d_0 = 2r_0 = (w/\pi) - \ell$.

e For the magnetron the r_0/ℓ values are such that the voltage pulses for these hollow-cylinder units would deviate appreciably from the desired flat-topped shape. If the wall thickness ℓ were decreased and the radius r_0 increased (keeping A fixed) r_0/ℓ would increase but τ would decrease. The time parameter RC/τ would then be larger than 0.15 still leading to appreciable deviation from flat-topped shape.

f Calculated using a density of 7.58 Mg/m³ for PZT 56:44.

g Calculated using Equation (83).

h τ reasonably small.

the expressions for the rectangular and hollow-cylinder units, respectively. At $t = \tau$, the voltage expressions for the two geometries are the same. The expression is

$$V = \frac{P_0 A}{C + C_L} \quad , \quad t = \tau .$$ (86)

Table 3. Energy converters with capacitive input impedances.[13]

Converter	Input Capacitance C_L (nF)	Input Voltage V (kV)	Operating Frequency (MHz)
Pancake (LC) Oscillator	1 - 300	500 - 5000	0.5 - 50
Spiral Oscillator	1000 - 10000	10 - 50	–
Frozen-Wave Generator	0.1 - 10	20 - 100	10 - 1000
Ross Circuit	0.01 - 1	20 - 100	10 - 16000
Transmission Line Oscillator	0.01 - 1	20 - 100	50 - 1000

The height of the PZT unit is given by Equation (80). The capacitance C of the unit is given by Equation (83). Substituting Equation (80) into Equation (83) gives

$$CV = 0.038A$$ (87)

47

with C in nF, V in kV, CV in μC, and A in mm^2. Substituting Equation (87) into Equation (86) gives an expression for the area A. The result is

$$A = 4.72\,C_L\,V \qquad\qquad (88)$$

with C_L in nF and $C_L V$ in μC. Using the value for C_L and V from Table 3, the size of the PZT unit can be estimated from Equations (80) and (88). The ratio C_L/C can be obtained by dividing Equation (87) by Equation (88). The result is

$$\frac{C_L}{C} = 5.56 \;. \qquad\qquad (89)$$

Table 4 gives the PZT geometrical size estimates for the capacitive energy converters. The thickness ℓ was taken as 12.6 mm with a corresponding pulse duration of 2.7 μs (as for the converters with resistive input impedances). The input capacitances and voltages cover the range of values listed in Table 3. Since $r_0/\ell \gg 1$ both the rectangular and hollow-cylinder units give the same response for all the cases shown. Table 4 indicates that the PZT units for the maximum input characteristics for the pancake and spiral oscillators are unreasonably large for power supply fabrication. It may be possible to fabricate the required PZT power supplies for the other listed input characteristics, but in some cases it may be impractical. For the spiral oscillator, with input characteristics of 1000 nF and 10 kV, it may be possible to fabricate a power supply by stacking a series of hollow-cylinder units (each 5 mm in height) that are electrically in parallel, each separated with a thin layer of insulating material. The 0.75-mm width of the PZT unit for the frozen-wave generator and Ross circuit with input characteristics of 0.1 nF and 20 kV is probably impractical and unnecessary. If the input voltage were increased to 100 kV the width would increase to a more reasonable value of 3.7 mm. For both the resistive and capacitive input impedance converters, it may also be possible to achieve a multishot power supply capability via the sequential depoling of multiple units.

Table 4. Estimated geometrical and electrical characteristics of PZT units for energy converters with capacitive input impedances.

Energy Converter	Input Capacitance C_L (nF)	Input Voltage V (kV)	Pulse Duration τ (μs)	Unit Height h^a (mm)	Unit Length ℓ^b (mm)	Unit Width w^c (mm)	Unit Area A^d (mm²)	Inner Cylinder Diameter d_0^e (mm)	Geometrical Ratio^f r_0/ℓ	Unit Volume (cm³)	Unit Mass^g (kg)	Unit Capacitance C^b (nF)	Unit Charge $P_0 A$ (μC)	Ratio C_L/C
Pancake (LC) Oscillator	1	500	2.7	250	12.6	190	2400	47	24	590	4.5	0.18	590	5.56
	300	5000	2.7	2500	12.6	5.6×10^5	7.1×10^6	1.8×10^5	8.9×10^4	1.8×10^7	1.3×10^5	54	1.8×10^6	5.56
Spiral Oscillator	1000	10	2.7	5	12.6	3700	4.7×10^4	1200	590	240	1.8	180	1200	5.56
	10000	50	2.7	25	12.6	1.9×10^5	2.4×10^6	6.0×10^4	3.0×10^4	5.9×10^4	450	1800	5.9×10^5	5.56
Frozen-Wave Generator	0.1	20	2.7	10	12.6	0.75	9.4	–	–	0.094	7.2×10^{-4}	0.018	2.4	5.56
	10	100	2.7	50	12.6	370	4700	110	53	240	1.8	1.80	1200	5.56
Ross Circuit or Transmission Line Oscillator	0.1	20	2.7	10	12.6	0.75	9.4	–	–	0.094	7.2×10^{-4}	0.018	2.4	5.56
	1	100	2.7	50	12.6	37	470	–	–	24	0.18	0.18	120	5.56

^{a}Calculated using Equation (80).

^{b}Taken as 12.6 mm.

^{c}Calculated using w = A/ℓ.

^{d}Calculated using Equation (88).

^{e}Inner diameter of hollow-cylinder unit having a cross-sectional area A, height h, and a wall thickness ℓ = 12.6 mm. $d_0 = 2r_0 = (w/\pi) - \ell$. For those cases in which no value is listed the area A is less than $\pi\ell^2$.

^{f}Hollow-cylinder units will give the same response as rectangular units since $r_0/\ell \gg 1$.

^{g}Calculated using a density of 7.58 Mg/m³.

^{h}Calculated using Equation (83).

VI. SUMMARY

Electrical equations have been derived for the normal-mode shock-depoling of PZT ferroelectric ceramics with resistive, capacitive, and inductive loads. To simplify the analysis, it was assumed that the PZT material responded in an ideal manner; i.e., charge was released completely and instantaneously at the shock front. Rectangular and hollow-cylinder shapes were considered for the PZT unit. Electrical expressions were obtained for the charge, voltage, current, and energy in the circuit as the shock front passed through the PZT unit and after the shock front passed out of the unit. Plots of these equations were presented as the magnitude of the load varied from short-circuit conditions to open-circuit conditions. These results and the electrical properties of shock-depoled PZT 56/44 ferroelectric ceramics were used to estimate the geometrical size and electrical characteristics of PZT units for selected energy converters with resistive and capacitive input impedances.

REFERENCES

1. W. Mock, Jr. and W. H. Holt, "Pulse Charging of Nanofarad Capacitors from the Shock Depoling of PZT 56/44 and PZT 95/5 Ferroelectric Ceramics," *Journal of Applied Physics*, Vol. 49, p. 5846 (1978).

2. P. C. Lysne and C. M. Percival, "Analysis of Shock-Wave-Activated Power Supplies," *Ferroelectrics*, Vol. 10, p. 129 (1976).

3. P. C. Lysne and C. M. Percival, "Electric Energy Generation by Shock Compression of Ferroelectric Ceramics: Normal-Mode Response of PZT 95/5," *Journal of Applied Physics*, Vol. 46, p. 1519 (1975).

4. W. Mock, Jr. and W. H. Holt, *Short-Circuit Current from the Axial-Mode Shock Depoling of PZT 56/44 Ferroelectric Ceramic Disks*, Naval Surface Weapons Center, NSWC TR-3781, Dahlgren, VA (January 1978).

5. P. C. Lysne, *Proceedings of the 6th AIRAPT International High Pressure Conference*, Boulder, CO, in press (1977).

6. W. J. Halpin, "Resistivity Estimates for Some Shocked Ferroelectrics," *Journal of Applied Physics*, Vol. 39, p. 3821 (1968).

7. J. T. Cutchen, "Polarity Effects and Charge Liberation in Lead Zirconate Titanate Ceramics Under High Dynamic Loads," *Journal of Applied Physics*, Vol. 37, p. 4745 (1966).

8. W. J. Halpin, "Current from a Shock-Loaded, Short-Circuited Ferroelectric Ceramic Disk," *Journal of Applied Physics*, Vol. 37, p. 153 (1966).

9. P. C. Lysne, "Dielectric Properties of Shock-Wave-Compressed PZT 95/5," *Journal of Applied Physics*, Vol. 48, p 1020 (1977).

10. P. C. Lysne and L. C. Bartel, "Electromechanical Response of PZT 65/35 Subjected to Axial Shock Loading," *Journal of Applied Physics*, Vol. 46, p. 222 (1975).

11. P. C. Lysne, "Resistivity of Shock Wave Compressed PZT 95/5," *Journal of Applied Physics*, Vol. 48, p. 4565 (1977).

12. P. C. Lysne, "Prediction of Dielectric Breakdown in Shock-Loaded Ferroelectric Ceramics," *Journal of Applied Physics*, Vol. 46, p. 230 (1975).

13. The electrical characteristics for the converters were provided by T. L. Berger, Electronics Systems Department, Naval Surface Weapons Center.

DISTRIBUTION

Commander
Naval Sea Systems Command
Washington, DC 20360
ATTN: SEA-0331 S. J. Matesky
           SEA-0332 W. W. Blaine
           SEA-0332 R. A. Bailey
           SEA-035 G. N. Sorkin
           SEA-0352 M. A. Kinna
           SEA-65313C L. H. Hawver

Commander
Naval Air Systems Command
Washington, DC 20360
ATTN: AIR-310 H. J. Mueller
           AIR-310B J. W. Willis
           AIR-320 T. F. Kearns
           AIR-350 E. M. Fisher
           AIR-350D H. B. Benefiel
           AIR-5324 S. Englander

Commander
Naval Weapons Center
China Lake, CA 93555
ATTN: R. L. Ballenger

Director
Army Ballistics Research Laboratories
Terminal Ballistics Laboratory
Aberdeen Proving Ground, MD 20015
ATTN: G. E. Hauver
           G. Moss

Commander
Army Materials and Mechanics Research Center
Watertown, MA 92172
ATTN: D. T. Dandekar
           J. F. Mescall